On the relationship between the water mass pathways and eddy variability in the Western Mediterranean Sea

E.K. Demirov

Department of Physics and Physical Oceanography, Memorial University of Newfoundland, St. John's, NL, Canada

N. Pinardi

Bologna University, Corso di Scienze Ambientali, Ravenna, Italy

Istituto Nazionale di Geofisica e Vulcanologia, Bologna, Italy

E. K. Demirov, Department of Physics and Physical Oceanography, Memorial University of Newfoundland, St. John's, NL, A1B 3X7, Canada (entcho@physics.mun.ca)

Abstract.

The role of eddies on the formation and spreading of water masses in the Western Mediterranean Sea is studied with an ocean general circulation model. The model is forced with interannually variable surface forcing for the years from 1979 to 1999. It is found that the model reproduces the major features of the observed mesoscale variability in the Gulf of Lions and the large eddies evolution in the Algerian Basin.

The seasonal evolution of circulation in the Gulf of Lions and processes of spreading of newly formed intermediate deep waters in the post-convection period is studied for years 1987 and 1992. The model results are compared with available for these years data from observations. It is shown that the instability of the transition zone between old and newly formed deep waters, which takes place after the violent mixing stages of the deep convection, leads to collapse of the mixed patch and formation of mesoscale eddies. Some of these eddies propagate out of the Gulf of Lions transporting deep waters into the Algerian Basin. The rest of the mesoscale eddies filled with newly formed deep waters remain in the Gulf of Lions, and tend to merge and enlarge. After the cyclonic eddies reach the Algerian Basin they interact with the intense mesoscale field existing there.

The energy analysis shows that the winter and spring are seasons of intensified baroclinic instability of the mean flow in the two regions of interest - the Gulf of Lions and Algerian Basin. The kinetic energy released by the processes of baroclinic instability is cascaded in spring and summer to-

wards small wave numbers. The spring spectra in the two regions have maximums at horizontal scales of about 80-100 km which is the typical scale of the eddies in the model. These eddies propagate a cyclonic circuit. The resulting eddy-induced mass transport is directed from the Gulf of Lions towards the Gibraltar Strait. Equivalently we can argue the intermediate and deep waters conveyor belt of the WMED is eddy driven.

1. Introduction

The processes of the water mass formation and transport in the Western Mediterranean (WMED) were intensively studied during the recent two decades. A comprehensive review of this work is given in Millot (1987, 1994, 1999), where the circulation features of the WMED and their role on the water mass transport are discussed mainly from an observational point of view. It was demonstrated in particular that the mesoscale variability has an important impact on the water mass transport in the WMED. At the same time the available data are rather sparse in time and space and some important questions about the water mass transport in the WMED remain still open. In particular, it is well known that the Mediterranean outflow to the North Atlantic involves waters which are formed by the deep convection in the Gulf of Lions (Kinder and Parilla, 1987). However their pathway from the north-west WMED to the Strait of Gibraltar is still not well studied (see Schott *et al.* 1996 for more discussions).

In this paper we study the impact of the eddy variability on the processes of formation and propagation of the WMED water masses by using an ocean general circulation model. Four WMED water masses will be of particular interest in our study - the Modified Atlantic Water (MAW), the Modified Levantine Intermediate Water (MLIW), the Winter Intermediate Water (WIW), and the Western Mediterranean Deep Water (WMDW). The surface characteristics in the basin are strongly influenced by the MAW, which originates from the Atlantic waters inflow through the Gibraltar Strait and propagates eastward along the African coast (see Fig. 1). The MAW occupies usually the upper 100 m layer and is characterised by salinity in the range from 36.5 psu at Gibraltar and 38 - 38.3 psu

in the northern WMED, and by temperatures below the mixed layer of about $14^o - 15^o$C (Millot, 1999). The Levantine Intermediate Water (LIW) forms in the eastern most part of the MED and enters the WMED through the Sicily Straiti (see Fig. 1), where it has salinity of about 38.7 psu and temperature maxima higher than 14^oC. In the WMED this water mass, which will be referred hereafter as the Modified Levantine Intermediate Water (MLIW), propagates at intermediate layers, and transforms due the processes of vertical and horizontal mixing. The MLIW follows a counter clockwise circuit in the Tyrrhenian Sea and through the Sardinia channel enters the Ligurian-Provencal Basin.

The WIW and the WMDW form during the winter convection in the northern WMED. The WIW, which has an important impact on the variability of the WMED (Millot, 1999), is defined by Salat and Font (1987) as water mass with temperature between 12.5^oC and 13^oC and salinity 38.1-38.3. The WIW is thought to be formed on the continental shelves and propagate in the whole basin below the MAW (see Pinot*et al.*, 1995). The WMDW formation in the Gulf of Lions (see Fig. 2) was observed by the MEDOC experiment (MEDOC group, 1970) in early 1969. Since that time several more observational studies reported deep waters formation in the region $3^o30'E \leq \lambda \leq 6^oE$; $41^oN \leq \varphi \leq 43^ON$, which now is commonly referenced as the MEDOC area (see Gascard, 1978). The deep convection usually reaches great depths over the local topographic feature of the Rhone fan (see Fig. 2) due to strong winter heat losses and specific local oceanographic factors which destabilise the water column.

The spreading of the water masses in the WMED, including those which form in the WMED (the WIW, and the WMDW) and those which enter the WMED through the straits of Sicily (the MLIW) and Gibraltar (the MAW) depends in a complex way upon

the variability of the circulation in the basin. The physical processes, which determine the transport and transformation of the water masses in the WMED are related to three different and interactive scales of the circulation in the MED (see Robinson and Golnaraghi, 1994), which are the basin scale, sub-basin scale and mesoscale. The basin scale circulation of the MED, which is shown on Fig. 1, is composed of one zonal thermohaline cell in the whole basin and two meridional thermohaline cells in the WMED and EMED respectively. The zonal cell is formed by the surface eastward flow of MAW and a westward transport of LIW in the EMED and the MLIW in the WMED at intermediate layers. The two meridional cells are driven directly by the processes of deep convection in the Gulf of Lions in the WMED and in the Adriatic Sea in the EMED respectively. Recently the EMED meridional cell received a contribution from the Aegean Sea deep waters, also called the Eastern Mediterranean Transient (Roether *et al.*, 1996).

The sub-basin scale circulation of the MED is composed of boundary currents, open ocean jets and gyres. A major sub-basin scale boundary current in the WMED is the eastward Algerian Current (AC) along the African Coast. This current reveals a relatively intense mesoscale variability (see Ayoub *et al.*, 1998), which may have an important impact on the MAW and MLIW spreading in the WMED (Fuda *et al.*, 2000; Millot and Taupier-Letage, 2005). A major sub-basin scale gyre is the Gulf of Lions cyclonic gyre in the northern part of the basin. The latter is composed in its northern part of the Ligurian-Provencal current (LPC) along the coastal shelf break of the Ligurian-Provencal basin and the Catalan Sea (Millot, 1999). In the south, the Gulf of Lions gyre is delimited by the Balearic current which hugs the northern side of the Balearic Islands (Pinot *et al.*, 2002). Eastward of the Balearic islands the current limiting the gyre gyre has not

been well defined in the literature except for the West Corsica Current (Millot, 1999) that closes the gyre in its eastern side. It is worth mentioning that also the western border of the gyre is not well defined probably because the mesoscale variability is very intense and makes it difficult to recognize a true western border. The previous model and data studies showed that the mesoscale variability in the Ligurian-Provencal basin strongly influences the processes of the WMDW formation and spreading, thus revealing a strong interaction with the basin scale and sub-basin scale circulation (see Swallow and Caston, 1973; Gascard, 1978; Madec *et al.*, 1996).

In this article we study the processes of deep and intermediate waters formation and spreading in the WMED, the impact of the eddy variability on the deep and intermediate water mass pathways and on the basin scale zonal and meridional circulation shown in Fig. 1. Detailed review of previous studies of these problems may be found in Marshall and Schott (1999) and Millot (1999). Throughout the text we will use these articles in the verification and interpretation of our results.

In our study we use an ocean general circulation model (OGCM), which is set up for the whole Mediterranean Sea and is forced by interannually variable surface momentum and heat fluxes (see section 2). In section 3 we compare the model results and available data about the deep convection in the Gulf of Lions. Section 4 describes the post-convective variability of circulation in the MEDOC area. In section 5 we discuss the mesoscale variability in the Algerian Basin as simulated by the model. Section 6 presents results about the physical processes of eddies generation and energetics. In section 7 we discuss the impact of the mesoscale variability on the water masses formation and transport.

2. The model

The model used is the Modular Ocean Model (MOM), with horizontal resolution of $\frac{1}{8}^o \times \frac{1}{8}^o$ and 31 vertical levels. The model set up, which is described in details in Demirov and Pinardi (2002), is based on the previous works of Roussenov *et al.* (1995) and Korress *et al.* (2000). Horizontal mixing is biharmonic with tracers coeffiecients equal to 1.5x10$^{10}m^4/s$ and the viscosisty coefficient is 5x10$^9m^4/s$. The vertical mixing is parameterized by constant vertical turbulent coefficients 0.3x10$^{-4}m^2/s$ for tracers and 1.5x10$^{-4}m^2/s$ for momentum. A standard convective adjustment is used to remove the static instability in the water column.

The surface forcing is computed in an interactive way with 6 hourly ECMWF (European Center for Medium Range Weather Forecast) atmospheric reanalysis and analysis fields and Sea Surface Temperature (SST) from the model (see Castellari *et al.*, 1998, 2000). The ECMWF reanalysis is used for the period 1979-1993 and ECMWF analysis for 1994 - 2000. The model is first run for 7 years with perpetual monthly mean forcing to reproduce the seasonal cycle in the basin.

The model results are from two different model runs - the first one for the period from 1979 to 1993, and the second one from 1993 to 1999. The two runs are initialized by the solution of the perpetual run. In a previous the paper Demirov and Pinardi (2002) presented model simulations with this model for the period of time from 1979 to 1993. The analysis of model results indicated in particular, presence of a large drift in the solution for the intermediate and deep layers. In order to diminish the effect of the model drift on the results for the years 1993 to 1999, the second simulation is initialized on January 1, 1993 by the solution of the perpetual run.

3. Deep convection in the Gulf of Lions: model simulation of the 1987 and 1992 events

In this section we analyze the model results for two particular years - 1987 and 1992. Extensive descriptions of the deep water formation in the Gulf of Lions for these years are available from the previous studies of Schott and Leaman (1991), Leaman and Schott (1991), and Schott *et al.* (1996). These authors showed that the surface forcing was different in the winters 1987 and 1992. Therefore we use the results from these works to verify how well our model results represent deep convection in the Gulf of Lions under strong (in year 1987) and weak (in year 1992) surface winter atmospheric forcing.

The data (Leaman and Schott, 1991) and our model simulations suggest that in 1987 the violent mixing phase of deep convection occurred in the Gulf of Lions already in late January. Thus we discuss the preconditioning phase for the beginning of January 1987 when model solution for the density field (Fig. 3) still does not indicate presence of deep convection. In Fig. 4 are shown velocity and density fields for the same depths and period, i.e. 1-3 January, but for year 1992. The circulation in the surface and intermediate layers over the shelf slope of the Gulf of Lions, is dominated by the LPC during the two years, 1987 and 1992 (see Figs. 3a,b, and 4a,b). A local intensification of the cyclonic flow is observed in the area over the Rhone fan, where a cyclonic vortex (C1) forms during the preconditioning phase. It is stronger in 1992 (Fig. 4a) and relatively weak in 1987 (Fig. 3a). For the two years the vortex C1 is hardly seen below 1000m (see Figs. 3c,d, 4c,d).

Previous studies noticed that the presence of C1 mesoscale vortex in the surface layer, which is exposed to the surface cooling, has an important impact for the deep convection.

Swallow and Caston (1973) observed this intense cyclonic vortex during the preconditioning phase of the deep convection in MEDOC area. Madec *et al.* (1996) reproduced the vortex in their numerical simulations of the Gulf of Lions, and showed that it has an important impact on the deep convection. Legg and McWilliams (2001) demonstrated, that even in the case of horizontally homogeneous surface forcing the deep convection area tends to localize in areas with relatively small horizontal extensions in the central part of the mesoscale vortices.

In the case of the MEDOC area the presence of the cyclonic vortex C1 is an essential component of the preconditioning, which determines the location of deep convection. It modifies the density field, producing a relatively strong uplifting of the ispycnal surfaces during the three years in the upper 1000 m in its central part (see Figs. 3a,b,c and 4a,b,c). The preconditioning of the water column and the strong Mistral winds in the area of vortex C1, which is very close to the Rhone valley, makes the conditions there most favourable for the violent mixing phase of the deep convection.

Beyond the vortex over the Rhone fan, two other mesoscale eddies (C2 and C3), which form by the instability of the cyclonic LPC are observed in 1987 and 1992 north-eastern and and south-eastern of the Rhone fan (see Figs. 3c,d and 4c,d). In opposite to the vortex C1, these eddies are well developed also at intermediate and deep layers (see Figs. 3b,c,d, and 4 b,c,d). We will refer these cyclonic eddies hereafter as the deep cyclonic eddies of the MEDOC area.

The density distribution during the preconditioning phase reveals some differences in the surface and deep layers. In the surface and intermediate layers the density gradients during the two years are strongest in the area of the Balearic front (Figs. 3a,b, 4a,b).

At depth 2000 m the area along the south-western boundary of the old WMDW in the MEDOC area is the zone of highest horizontal density gradients instead. The circulation inside the area of old WMDW bounded by this front is dominated by the deep cyclonic eddies (Figs 3c,d, 4c,d) , which have a relatively weak signal at the surface (Figs. 3a,b, 4a,b).

Even though they have variable size and positions, the three eddies (C1, C2, C3) tend to persist during the two years. They are positioned inside the Gulf of Lions cyclonic gyre and show some relation to the topographic features. C1 forms always over the Rhone fan. The deep cyclonic eddies C2 and C3 develop in the two deep areas within the cyclonic gyre and separated by the Rhone fan. The physical processes of formation of these eddies are discussed in more details in sections 4 and 6.

The observational studies of Schott and Leaman (1991) and Schott *et al.* (1996) indicated that the deep convection in 1987 and 1992 had a different intensity and horizontal extension. The shaded area on the upper pannel of Fig. 5 shows the horizontal extension of the mixed patch in 1987, where the water column was homogenized down to depths of 2000m (see Fig. 5, lower pannel). In the 1992 the convection was observed in a small area (see Fig. 6, upper pannel) and down to 1500 - 1800 m depth only (see Fig. 5, lower pannel). A vertical meridional section of the model density distribution along the 5^oN is shown on Fig. 7 for the "violent mixing" phase of the deep convection events in 1987 and 1992. The position of the deep convection in the two cases is concomitant with the position of cyclonic vortex C1 over the Rhone Fan on Figs. 3a, 4a. The density distribution suggests that the water column in the MEDOC area is homogenised in 1987 down to 2000m depth (see Fig. 7a). In 1992 (see Fig. 7b) the vertical mixing reaches maximum

depths only of about 900m. The position and depth of deep convection in 1987 in the model results correspond well to the observations of Leaman and Schott (1991) for 1987 (Fig. 5). The model underestimates the depth of the deep convection in 1992 (see Fig. 6) and the density of newly formed deep waters in the two years. Castellari et al, 2000 showed that the intensity of the deep convection and the properties of newly formed deep water are strongly sensitive to the uncertainties in the surface forcing. The ECMWF reanalysis which we use as forcing our model study has horizontal resolution of about 100km. The comparison with at sea meteorological observations show that the ECMWF ERA2 surface fluxes tend underestimate the intensity of the surface forcing(Castellari personal communication). The error in the characteristics of newly formed deep water is a result of uncertainties in the surface forcing. At the same time this error (of about 0.05) is relatively small with regard to the horizontal contrast of density created by the deep convection and we assume that it is not significant for the post-convective evolution of the circulation in the MEDOC area which is discussed in the following sections.

4. Post-convective variability of the MEDOC area

The two deep convection events in 1987 and 1992 had different intensity. Correspondingly our mode results suggest that the post-convective evolutions of the newly formed deep waters in these two years were also different. Here we use the model results from the 1987 run to study the post-convective evolution of newly formed WMDW. The results from the 1992 simulations are used to identify the changes in the regime of circulation in the Gulf of Lions during the years of weak winter convection (1992) with respect to the circulation in years of intense formation of the WMDW (1987).

The homogenization of water column during the violent mixing stage, which diminishes the Rossby radius of deformation, favors baroclinic instability of the flow (see Legg and McWilliams, 2001). The flow during the first days and weeks after the deep convection is dominated by relatively small eddies (not shown here) which tend to merge and enlarge.

In March, 1987 some small eddies with size of few tens of km are still observed in the velocity and density fields (see Fig. 6a) but the flow is generally dominated by the large scale cyclonic LPC. An eastward branch of LPC forms during this year at latitude of about 41.5^oN. This branch gives an origin of a cyclonic rim current, which runs around the mixed patch, and along the zone of the highest horizontal density gradients at surface and intermediate layers. The latter is commonly referenced also as transition zone (Testor and Gascard, 2003). The rim current is very weak and almost not present during the year 1992 when the intensity of the winter convection was relatively weak (Fig. 9a). The surface density and velocity fields evolution during the consequent months (Figs. 8b-8f and 9b-9f) reveal two major tendencies: a) weaken of the horizontal density anomalies in the MEDOC area due to the surface heating; and b) intensified intrusions of MAW from the Algerian Basin along the Western Corsica coasts and intensified the Balearic front. These tendencies lead to the intensification of the circulation along Balearic front and of the Western Corsica Current.

The rim current is the dominant circulation feature in the intermediate layer during the months March - May of 1987 (Figs. 10a,b). Though the instability of the cyclonic rim current and mesoscale eddies produce lateral outflow, the area of the newly formed dense intermediate waters remains compact until June, 1987. Thus the mixed patch at intermediate layers tends to persist in the model solution until early summer. In 1987

the mixed patch breakdown in July and splits in several smaller eddies. In following months, the eddies in the south-eastern part of the mixed patch tend interact and merge with surrounding eddies . As a result a new eddy (C4) forms at the southern edge of the MEDOC area, which in October (Figs. 10e,f), tends to propagate southward in to the Algerian Basin (see also section 6). The eddies which form after the collapse of the mixed patch in its northwestern part tend to merge and enlarge, and organizing into a new area with cyclonic but weaker circulation. In 1992 (Fig. 11), when the winter convection is relatively weak and newly formed intermediate waters are of relatively small amount, the above described features of density and velocity distributions are not well represented. During this year the area of newly formed intermediate waters split in two smaller areas already in April and then slowly dissipate due to the lateral exchange.

The circulation in the deep layers in March of 1987 (Fig. 12a) indicate presence of the south-eastern part of the rim current. Its position corresponds well to the transition zone in the intermediate layer. This current is less stable than in the intermediate layers and already in April, May (Figs. 12b,c) two intense mesoscale eddies form in the area of newly formed waters at the position close to that of eddies C2 and C3 observed during the preconditioning phase. These two eddies dissipate together with the collapse of the mixed patch in July (Figs. 12d) and the newly formed deep waters partly mixes with the surrounding waters and partly remain captured by the newly formed smaller eddies. One of these eddies is the C4, which then propagate southward, bringing the WMDW towards the Algerian Basin.

5. Simulated eddy variability in the Algerian Basin

The Algerian Basin (see Fig. 2) is the region where the WMDW outflow can occur after the convection processes. This implies a meridional circulation of the WMDW, as depicted on Fig. 1. The transport by the sub-basin scale currents and gyres and the mesoscale eddies in the Algerian Basin compose the conveyer belt in this part of the WMED. The recent studies showed that the Algerain Current, which is a major sub-basin scale current that conveys the MAW westward, reveals a strong mesoscale variability. According to Fuda *et al.* (2000) "the Algerian Current generally appears as a series of eddies, mainly anticyclonic a few 10 of km in diameter, propagating downstream at 3-5 km/day". Millot *et al.* (1997) defines two kinds of mesoscale eddies of the Algerian Current. Most of the Algerian eddies are relatively small, with few tens of kilometers horizontal extension, and shallow, only in the surface 200 m layer. Following Fuda *et al.* (2000) we will refer them as *serial* or *surface eddies*. They have a strong signal only in the velocity field of the surface MAW. The second kind of Algerian eddies called *events* (Fuda *et al.*, 2000) are deep and induce strong currents at all depths. In the coastal area of Algerian Basin, events often have a complicated vertical structure and 100 - 200 km horizontal size (Fuda *et al.*, 2000). Near the African coast, the events tend to propagate eastward, and approaching the Sardinian channel they turn northward (Millot, 1985; Vignudelli, 1997). Then they move back westward in to the deep part of the basin (Benzohra and Millot, 1995; Millot *et al.*, 1997). The propagation of these events along this cyclonic circuit may last as long as 3 years (Puillat *et al.*, 2002).

Here we discuss the simulated eddy variability in the Algerian Basin for the period of 1997 and 1998. This particular period was chosen because it covers the time period of the ELISA-4 experiment in the Algerian Basin (see Millot and Taupier-Letage, 2005).

During this time period two of the eddies are relatively persistent and following Millot and Taupier-Letage (2005) they will be refereed here as eddy 96.1 and eddy 97.1 (see Fig. 13).

In the model solution, the eddies of the AC are predominantly anticyclonic. Fig. 14 shows the temperature and velocity fields in the surface layer averaged over four 3 days periods of time. During the first period 27-30 July, 1997 (see Fig. 14a) the eddy 97.1 in the model is at position southern of Balearic Islands. Millot and Taupier-Letage (2005) observed during July, 1997 two anticylonic eddies, which they named as 96.1 and 96.2, interacted western of Sardenia (see Fig. 13). In the model solution this structure is present (see Figs. 14, 15), which is somehow shifted eastward with respect to the observations. During 1998 three anticyclonic eddies dominate the structure of the velocity field in the Algerian Basin. Two of them are persistent and are present during the whole period (eddies 96.1 and 97.1 in Millot and Taupier-Letage,2005). A third anticyclonic eddy 96.2 is observed in the northern part of the Algerian Basin during the whole 1998. It is not reported in the study of Millot and Taupier-Letage (2005) because the data set used in their study did not extend towards this region. According to the observations (see Figs. 13d,f,h) the anticyclonic eddies 96.1 and 97.1 propagate during the period March-June, 1998 with velocites, which are higher than their estimations by the model (see Figs. 14b,c,d, and Figs. 15b,c,d)). However, we should mention that the long-term identification of these eddies is somehow problematic due to the fact mentioned by Millot and Taupier-Letage (2005), that the messocale eddies of the Algerian Basin tend continuosly to interact, merge and split into smaller eddies. Therefore the positions of eddies defined by data and model include an error. At the same time, beyond the

reported differences between the model and data, the intercomparions indicates that the model predicts well the size, type, life time and the general direction of propagation of the eddies in the Algerian Basin.

Comparing the surface fields (Figs. 14) with that at intermediate layers (Figs. 15) one can remark that the anticyclonic eddies in the western part of the Argerian Basin are surface intensified and there they are relatively weak at intermediate layers. Moving eastward these eddies intensify also at intermediate layers. The strongest eddy induced currents at intermediate layers are observed when the anticyclonic eddies approach the western coast of Sardinia. This intensification of intermediate circulation is concomitant with the process of trapping by the eddies of MLIW, which enter the Algerian Basin through the Sardinia Channel. Going northward along the Sardinia coast the anticyclonic eddies remain strong at intermediate layers and weaken at the surface. This is very well seen in the eddy 96.1, which in western Algerian Basin in July 1997 (see Figs. 14, 15), is very strong at the surface and weak at intermediate layers. Approaching the Sardenia Channel This eddy intensifies also at intermediate layers (see Figs. 14, 15). The eddy 96.2 which is in the northern part of the Algerian Basin in 1998 gradually weakens at the surface and intensifies at intermediate layers from March to June.

6. Eddies of the Algerian and Provencal Basins: generation, scales, and energetics

In the previous sections we have discussed two different aspects of the eddy variability in the WMED. The first one is related to the processes of deep water formation in the MEDOC area and spreading of the WIW and MWDW, and the second one is related to the mesoscale variability in the Algerian Basin. These two problems, which are com-

monly studied separately, reveal many similarities and interconnections. In particular, the variability of the two areas - the northern WMED and the Algerian Basin are strongly influenced by the mesoscale eddies. This result is also supported by existing observational studies discussed above. In this section we discuss the physical processes that govern the generation and evolution of WMED eddies.

The sinking and spreading, which occurs after the violent mixing, is the less studied stage of the deep convection in the MEDOC area. During this stage the newly formed deep waters propagate outside the MEDOC area. Previous model (Jones and Marshall, 1993; Madec *et al.*, 1991, 1996) and observational (Gascard, 1978) studies suggest that the mesoscale eddies generated by the instability of the rim current play an important role for the mixing between the area of deep convection and the stratified waters outside the region of deep convection. The model results discussed in section 4 suggest also that the processes of geostrophic adjustment, baroclinic instability and mixed patch breakdown have a strong impact on the mixed patch water masses spreading. In particular our model results show that the mixed patch is relatively stable during the spring and only in early summer it breakdowns into several eddies. Similar conclusion about the post-convective behavior of the mixed patch is made in the previous studies of Legg and Marshall (1993, 1998). These authors demonstrated that the mixed patch formed after the deep convection tends to break down into mesocale "clumps", which transport efficiently the newly formed cold waters away from the deep convection areas. Legg and Marshall (1993) have shown that when the rim current is not present the mixed patch breaks down on time scale of few days. The presence of a strong cyclonic rim current, however, significantly influences the dynamics of the mixed patch. In particular, Madec

et al. (1996) demonstrated that the barotropic cyclonic current around the MEDOC area suppresses the baroclinic instability during the time period immediately after the deep convection. Legg and Marshall (1998) showed that this impact of the ambient flow on the stability of the mixed patch depends strongly on the intensity of the rim current. If the cyclonic flow is not strong enough, the baroclinic potential vorticity anomaly created by the deep convection continuously increases and generates baroclinic instability. If however the pre-existing barotropic potential vorticity anomaly is energetic enough, it may suppress the baroclinic instability. Legg and Marshall (1998) suggested that in this case the ambient cyclonic flow is "self-perpetuating", i.e. the cyclonic circulation inside the deep convection area reinforces the ambient flow, while the intensified rim current suppresses more efficiently the baroclinic instability. In our model simulations this "self-perpetuating stage" is observed in the post-convective development of the mixed patch before its breakdown in the beginning of summer. The model solution (see section 4) suggests that during this stage the eddies within the mixed patch tend to merge and enlarge and the cyclonic flow around the convection area intensifies during this stage.

From the discussion of the model results presented above it follows that the post-convective circulation in the Gulf of Lions reveals a strong interaction between the mean and eddy flow. In order to quantify the energy conversion between the eddy and mean flows here we estimate the rate of energy conversion between mean and eddy flow for the Gulf of Lions and the Algerian Basin. Tables 1-6 show a long term estimation of the mean (APEm) and eddy (APEe) Available Potential Energy, mean (KEm) and eddy (KEe) kinetic energy. Here we will also discuss the terms in the equations of energy balance which describe the conversion rate of APEm to APEe - T_1, which characterize

the intensity of the baroclinic instability and the conversion rate of KEm to KEe T_2. These elements of the energy balance are computed for the surface ($0m < z < 250m$), intermediatea ($250m < z < 500m$) and deep ($z > 500m$) layers.

The surface forcing over the WMED is strongest in the winter season. During this season there is a strong increase in the APEm for the two basins, the Algerian Basin and the Gulf of Lions. The increase of APEm in the Gulf of Lions is partly due to the intensified surface APE flux, and partly due to intensified conversion of KEm to APEm. In the Algerian Basin the major factor for the winter APEm increase is the intense lateral APEm advective flux through the Gibraltar Strait during this season. The transformation of APEm to APEe through the processes of baroclinic instability in the surface layer for the two regions is strongest also in winter (Table 1). In the intermediate and deep layers the seasonal variability of APEm is much smaller than in the surface layer. The baroclinic instability in these layers is strongest in the spring. The conversion of the kinetic energy of mean flow to eddy kinetic energy in all of the layers has a smaller impact on the generation of eddy energy than the processes of baroclinic instability. In some of the cases (like summer season in the Algerian Basin), the conversion term T_2 is directed from eddy to mean flow.

A more detailed discussion of the mean and eddy energy and energy conversions in the WMED is presented in Demirov and Pinardi (2006a) and in Demirov and Pinardi (2006b). From the results presented in Table 1 we may conclude that the dominant mechanism for the formation of mesoscale eddies in the WMED are the processes of baroclinic instability, which convert $APE_m \rightarrow APE_e \rightarrow KE_e$ and are strongest in winter and spring. The baroclinic instability in the surface layer of the Algerian Basin (Table 1)is much stronger

than that for the Gulf of Lions (Table 4). On the other side the eddy energy production by baroclinic instability in the intermediate and deep layers is much stronger in the Gulf of Lions (Tables 2,3) than in the Algerian Basin (Tables 5,6). The processes of baroclinic instability inject kinetic energy at scales dependent on the internal radius of deformation Ro. At the same time the model and data results discussed above show that the most energetic eddies in the WMED have horizontal scales larger than Ro. Here we discuss the processes that govern the eddy dynamics and spatial scales for year 1987. We calculate the energy spectrum for two regions, which are shown on Fig. 2).

The three days averaged spectrums of barotropic kinetic energy in the Gulf of Lions are shown on Fig. 16 for four periods of 1987: winter (JFM), spring (AMJ), summer (JAS) and autumn (OND). These periods coincide with the major stages in the evolution of the MEDOC area described in sections 3 an 4, i.e. 1) violent mixing in winter, 2) "self-perpetuating" stage of the post-convective evolution of the mixed patch in spring, 3) mixed patch breaks down in summer, and 4) spreading of newly formed deep waters in autumn. The kinetic energy spectrum is normalized to satisfy $\int_0^\infty E(k)dk = \overline{\frac{(u_b^2+v_b^2)}{2}}$, where $\overline{\frac{(u_b^2+v_b^2)}{2}}$ is the area mean kinetic of energy of vertically mean flow.

We should mentioned that the surface forcing during the considered period from 1981 to 1993 experienced a strong interannual variability. Correspondingly changed the energy of the flow (Demirov and Pinardi, 2002) and its spectrum. At the same time though the spectral densities varied during the whole period, there are certain spatial scales, which persistently dominated the velocity spectra, which are linked to the spatial and time variability of the flow discussed in sections 3 - 5. Here these scales and their connection to the seasonal flow dynamics are discussed for the case of year 1987.

Winter energy spectrum in the Gulf of Lions on Fig. 16a is characterized by high values of spectral densities in the whole spectral interval. During this season, the strong atmospheric forcing injects energy at large scales of order several hundreds of kilometers (which is not shown on the Fig. 16a. The strong variability in the surface forcing results in a high variance of the spectral curve values. This variance is relatively strong in high wave number interval $2\pi/k < 50km$.According to the linear instability theory for continuously stratified fluid, the fastest growing mode is at wavelength of $\gamma = 3.9Ro$, where Ro is the internal radius of deformation (see Cushman-Roisin, 1994). Ro during this season changes from 5 km during the period of winter convection to about 15 km at the beginning of the spring (see Robinson and Golnaraghi, 1994). Correspondingly the wave numbers of fastest growing modes evolve within the interval from 15km to 60km and the spectrum is highly variable within interval. This spectral interval will be refereed hereafter as to the *interval of baroclinic instability*. The spectrum variance within the interval instability is relatively high during the all seasons. During the period April-June (Fig. 16b) a spectral maximum develops at $2\pi/k_0 \approx 70km$. As discussed above during this season, the eddies generated within the mixed patch by the processes of baroclinic instability tend to merge, enlarge and intensify. Correspondingly the dominant scale in the energy spectrum also increases towards $2\pi/k_0$. The mixed patch in July collapsed into (section 4) smaller scale eddies. The spectral maximum at k_0 decreases during the the summer and at the end of the season it almost disappear (Fig. 16d). Correspondingly the spectral density increases at $2\pi/k_1 \approx 50km$ which is within the interval of baroclinic instability. During the period October-December the maximum at k_1 gradually disappear and a new spectral maximum developed wave numbers close to k_0.

The barotropic kinetic energy spectrum for the Algerian Basin (Fig. 17) reveals a similar shape. We recognize the same spectral intervals as on Fig 16: (1)the interval of baroclinic instability $60 < 2\pi/k < 15$; (2) the spectral maximum at $k_0 \approx 110km$. The scale $2\pi/k$ in the Alegiran Basin a slightly "shifted" towards the low wave numbers due to the fact that the Ro has higher values here than in the weakly stratified Gulf of Lions. As for the Gulf of Lions, the spectrum is highly variable in the interval of baroclinic instability. The variation of spectra in the in the interval $k_0 < k < k_1$ however is obviously lower than in the Gulf of Lions. In all of the seasons the spectrum in this interval is close to -5/3. This slope is predicted by the 2-D turbulence spectrum slope for the interval of inverse cascade.

The theory of 2-D quasi-geostrophic turbulence predicts that in a flat bottom f-plane ocean the energy-containing scales increase due to the inverse cascade until they reach the domain size. If however, there exists a mechanism restricting the size of the eddies, a kinetic energy peak develops at scales at which the inverse cascade halts (Laricheiv and Held, 1995). The mechanisms that may halt the inverse cascade are related to β-effect, scaterring by topography, or boundary layer friction. On β-plane, the inverse cascade is halted at the Rhines scale $k_R = (\beta/V)^{\frac{1}{2}}$ for which the velocity scale of eddies propagation V becomes equal to the Rossby waves phase speed (see Rhines, 1975). The definition of Rhines scale includes implicitly the assumption that at large scales there exist an efficient mechanism for dissipation of the energy cascaded towards k_R. Otherwise the energy in dissipation-free ocean flow would keep accumulating at k_R. The Rhines scale for the WMED is $2\pi/k_R \approx 500km$ and is larger than maximal horizontal extension of deep part of the basin, which is about 400 km (see Fig 2). Additionally the size of the eddies

in the Gulf of Lions and Algerian Basin are limited by to the processes of dissipation which depend in a complex way by the scattering by topography, lateral and bottom friction. The energy spectrum suggest that these processes halt the inverse cascade at about $2\pi/k \approx 70km$ in the Gulf of Lions and at about $2\pi/k \approx 110km$ in the Algerian Basin.

7. Mean and eddy induced transport in the WMED

The zonal cell of the thermohaline circulation in the WMED consists of a surface westward transport of MAW and westward transport of MLIW. While the Algerian Current and the paths of the surface MAW are well studied, the results from studies of the MLIW transport in the WMED and mechanisms of its formation are less known. In previous coarse resolution model and data studies, Ovchinnikov (1966), Wu and Haines (1995), Korres *et al*(2000) suggested that the MLIW are transported westward in the Algerian basin by a current which is in an opposite direction of the Algerian Current. According to the results of these authors this current, which is the Algerian Counter Current (ACC), may be present in the WMED with different intensity during the years. Some recent observational studies (see Fuda *et al.*, 2000) suggest that the ACC is not observed in high resolution and eddy resolving data. The long-term MLIW pathways according to these results depend strongly on the eddies propagation in the region, and especially on the existence of persistent paths of eddy propagation (see Millot and Taupier- Letage, 2005).

Our model results for year 1987 presented above show that the eddies with scale of about 100 km dominate the flow in the deep and intermediate layers of the WMED. One can anticipate under the conditions of relatively weak mean flow, the eddy-induced transport may potentially play an important role for the water mass spreading. At the same time

the simulations of 1992 suggest that during years with weak convection the eddy activity in the MEDOC are is also weak. Here we try to answer the question how strong is the eddy induced transport with respect to the mean mass transport.

The eddies influence the time-mean transport in two ways. One way is rectification of the mean flow. This effect of the eddies on the mean flow may be estimated if two simulations of fine- and coarse- resolution version of the same model and with the same forcing. Such a twin experiment has not been done with the present model and the rectification of the mean flow is not discussed here. We study only the second effect of eddies on the time-mean transport, which results from the correlation between density and velocity. The integral advective transport of σ_t for the layer $z_1 < z < z_2$ is given by:

$$\mathbf{U} = \int_{z(z_1)}^{z} \mathbf{u}\sigma_t dz \quad ,$$

consists of mean $\overline{\mathbf{U}}$ and eddy-induced $\mathbf{U}'$ components, where

$$\overline{\mathbf{U}} = \int_{z(z_1)}^{z} \overline{\mathbf{u}}\overline{\sigma}_t dz \quad ,$$

and

$$\mathbf{U}' = \int_{z(z_1)}^{z} \overline{\mathbf{u}'\sigma_t'} dz \quad .$$

Here $\overline{\mathbf{u}}$ and $\overline{\sigma}_t$ are the time mean fields of the velocity vector $\mathbf{u}$ and density σ_t and the $\overline{\mathbf{u}'\sigma_t'}$ is the velocity density correlation. Here we compute the mean $\overline{\mathbf{U}}$ and eddy induced $\mathbf{U}'$ transports for two layers: the intermediate layer between $250m < z < 500$, and the deep layer for $z > 500$. The stream functions for the mean and eddy induced mass transport in the two layers are then computed by inversion of the Laplasian operator $\nabla \times \mathbf{U}$, i.e.

$$\overline{\psi} = \nabla^{-2}\mathbf{k}.\left(\nabla \times \overline{\mathbf{U}}\right),$$

and

$$\psi' = \nabla^{-2}\mathbf{k}.\left(\nabla \times \mathbf{U}'\right),$$

where $\mathbf{k}$ is an unit vector directed upwards. At open boundaries, the stream function is defined as a line integral of the normal to the boundary component of $\overline{\mathbf{U}}$ and $\mathbf{U}'$ correspondingly. The mean and eddy-induced transports in the intermediate and deep layer are shown on (see Fig. 18).

The mean transport (Fig. 18a) in the intermediate layer of the Gulf of Lions is dominated by the cyclonic gyre, which is observed in the surface and intermediate layers of this region. An anticyclonic transport is present in the southeastern Gulf of Lions and eastern Algerian Basin. These two elements of the transport does not imply an outflow of intermediate waters out of the Gulf of Lions. The mean transport in the deep layer includes several areas of cyclonic and anticyclonic circulation. Some of these areas correspond well to the mesoscale variability discussed above. The two deep cyclonic eddies in the Gulf of Lions C2 and C3, which in 1987 and 1992 are present in the model solution with different intensity have a strong signal also in the mean transport. The same is true for the cyclonic circulation in the southeastern part of the Gulf of Lions. The circulation here is cyclonic mostly during the spring and summer when the eddy C4 tends to form. This area is relatively large as the area of the anticylonic eddy in the central part of the Gulf of Lions. The reason for that is that the position of C4 and the anticyclonic eddy in the Gulf of Lions in model solution is highly variably in contrast to the position of quasi permanent eddies C2 and C3. The position of C4 in particular is in the southeastern Gulf of Lions in winter and moves southward in the spring. In summer and autumn C4 is very weak. In this way beyond the cyclonic transport in the intermediate layer of the

northwestern Gulf of Lions, all the most intensive feature in the transport of intermediate and deep layers show influence of the eddies C2, C3 and C4 and the anticyclonic eddy, which often present in the Gulf of Lions.

The eddy-induced transport (Fig. 18cd) in the major part of intermediate and deep layers of the WMED is cyclonic during the whole year. It transports MLIW cyclonically, from the Sardinia Channel along the western coast of Sardinia, Corsica and then into the Gulf of Lions. The WMDW, WIW and MLIW are transported by the eddy-induced transport out of the Gulf of Lions along the eastern coast of the Majorca Island and then westward towards the Gibraltar Strait. An anticyclonic eddy induced transport in the southern part of Algerian Basin produces a westward transport of MLIW and WMDW but just in a narrow area along the African Coast.

These eddy-induced paths of the MLIW and WMDW in the model solution dominate over the mean mass transport and are consistent with existing observational data, which are reviewed in Millot and Taupier-Letage (2005), and Testor et al. (2005). In particular, the latter work of Testor at al.(2005) presents results from floats trajectories observations in the Algerian Basin. The trajectories, which are shown on Fig. 19 cover the southern region of the WMED. The data confirm presence of a cyclonic circulation in the Algerian Basin which has many similarities with the model eddy-induced transport on (Fig. 18cd). In the intermediate layer the observations show a presence of a cyclonic circulation in the area $4^oE < \lambda < 8^oE$ and $37^oN < \phi < 39^oN$ in a good agreement with the model solution (see Fig. 18c). In the deep layer the trajectories show the presence of cyclonic circulation in the area between $1^oE < \lambda < 9^oE$ and $37^oN < \phi < 39^oN$. The model suggests that a deep layer eddy induced cyclonic circulation is presented also in the northern part of the

Algerian Basin (Fig. 18d). The data in this area, however, are limited and the observed trajectories in this area does not allow to assess how realistic is this model result.

8. Discussions and conclusions

In this article we present the model results for the deep convection in the Gulf of Lions, mesoscale variability in the WMED and waters masses spreading. We tray to answer two major questions a) what are the processes of generation of intense mesosclae variability in the WMED; and b) what is the relatively role of mean and eddy induced transport on the formation of the conveyor belt in the WMED.

The analysis of the numerical results demonstrated that the model is capable to represent important features of the deep convection in the Gulf of Lions known from previous data and model studies. These are the modifications of the water column characteristics during the preconditioning phase, the violent mixing with different intensity depending on the interannual variability of the surface heat and momentum forcing and post-convective adjustment of the circulation in the area of mixed patch. We have studied two cases of deep convection in the MEDOC area, that of 1987 and 1992, when the intensity of the vertical mixing was different. In the model in 1987 the deep convection reached the bottom, while in 1992 the in the model solution it is just down to 800m. The comparison with the observations of deep convection during these years shows that the model tends to underestimate the density in the deep convection mixed patch and the deep convection depth in 1992. This model error is shortcoming of the uncertainties in the surface forcing and on our knowledge is common in the existing model simulations of the Mediterranean Sea.

The evolution of model solution during the third "sinking and spreading" phase of the deep convection was studied for the two cases: the years of 1987 with relatively strong deep convection, and the year 1992 with convection down to intermediate layers. The comparison of the circulation during these two cases suggests that circulation patterns differ significantly between years with and without deep water formation in the Gulf of Lions. In particular the adjustment processes after the formation of the mixed patch force a strong rim currents during the years with deep convection, which is weak and almost not present in the year 1992 when the winter convective mixing was relatively weak.

The model results suggest that the mixed patch formed during the deep convection is a stable feature, which persists during a period of several months after the deep convection events. During this time it extends at intermediate and deep layers and related to it rim current and mesoscale variability tend to intensify. This is not seen in the surface layer, where the density anomalies created by the winter convection and the rim current tend to weaken and disappear due to the spring waters restratification. In early summer the mixed patch, which at that time is mainly present in the intermediate and deep layers, collapses and splits in several cyclonic eddies. The cyclonic eddies in the south-eastern edge of the MEDOC area tend to interact, intensify and merge into a single eddy, which traps partly newly formed interemediate and deep waters and propagates towards the Algerian Basin in late autumn. The rest of the cyclonic eddies remaining in the MEODC area tend to merge and enlarge. The density gradients and newly formed rim current however are much weaker with respect to those immediately after the winter.

The energy analysis for year 1987 shows that the dominant process of mesoscale eddies in the WMED is the baroclinic instability. It is strongest in winter and spring, when the

available potential energy stored during the winter season is released in eddy potential and kinetic energy. At the same time the dominant spatial scale of the mesoscale eddies in the model solution (and available data) is about 100km and may reach in some cases 200km. This scale is larger than the length of the fastest growing mode, which is expected to dominate the eddies formed by the baroclinic instability. The analysis of seasonal spectra of barotropic energy for year 1987 in regions - the Gulf of Lions and Algerian Basin suggests that the mesoscale eddies with dominant scale of 100km is a result of inverse cascade. As mentioned above the release of eddy energy by the processes of baroclinic instability is strongest in winter and spring. In the spring and summer the eddies generated by the baroclinic instability tend to merge and enlarge towards the scale $(2\pi/k_0)$ of spectral maximum.

The comparison of mean and eddy induced transport suggests that the eddy induced transport prevails over the mean transport in the areas which are important for the spreading of WMDW and MLIW. Moreover, the circulation patterns in the mean transport in the Gulf of Lions are concomitant with eddies C2, C3, C4 observed in the 1987, 1992 model solution. Therefore we may consider the eddy-driven component of the water mass transport as an important part of the conveyor belt. This component, which we call eddy driven conveyor may potentially give the answer to the two questions which are widely discussed in the literature for the WMED: a) How MLIW propagate towards the Gibraltar if as show the observations the ACC, which was thought to be the major "transporter" of MLIW in the Algerian Basin, is not existing; and b) What is the mechanism of the WMDW transport towards to the Gibraltar. The eddy mean transport is the mechanism,

which is regularly present in the region and may bring effectively these waters outside the Gulf of Lions and/or westward in the Algerian Basin.

Acknowledgments. The work is contribution to the EU funded project MFSTEP and project 312377-05 funded by Natural Sciences and Engineering Research Council of Canada.

References

Ayoub, N., P.-Y. Le Traon, and P. De Mey, 1998, A description of the Mediterranean surface circulation from combined ERS-1 and TOPEX/POSEIDON altimetric data. *J. Mar. Syst.*, *18*, (1-3), 3-40.

Benzhora M., and C. Millot C., 1995. Characteristics and circulation of the surface and intermediate water masses off Algeria. *Deep-Sea Res.*, *42*,(10), 1803- 1830.

Buongiorno Nardelli, B., G. Larnicl, E.DÁcunzo, R.Santoleri, S. Marullo, and P.-Y. Le Traon, 2003. Near real time SLA and SST products durino 2-years of MFS pilot project: processing, analysis of the variability and the couplet patterns, *Ann. Geophys.*, *21*, 103-121.

Castellari, S., N. Pinardi, and K.D. Leaman, 1998. A model study of air-sea interactions in the Mediterranean Sea, *J. Mar. Syst.*, *18*: 89-114.

Castellari, S., N. Pinardi, and K. Leaman, 2000. Simulation of water mass formation processes in the Mediterranean Sea: Influence of the time frequency of the atmospheric forcing, *J. Geophys. Res.*, *105*, N 10: 24157 - 24181.

Danilov, S., and D. Gurarie, 2002. Rhines scale and spectra of the β plane turbulence with bottom drag., *Phys. Rev. E*, *65*, 067301,1-3.

Demirov, E., and N. Pinardi, 2006. Simulation of the Mediterranean Sea circulation from 1979 to 1993: Part I. Energetics of variability (in preparation)

Demirov, E., and N. Pinardi, 2002. Simulation of the Mediterranean Sea circulation from 1979 to 1993: Part I. The interannual variability. *J. Mar. Syst.*, *33-34*:23-50.

Fuda, J.L., C. Millot, I. Taupier-Letage, U. Send, J.M. Bocognano, 2000.XBT monitoring of a meridian section across the western Mediterranean Sea, *Deep-Sea Res.*, *47*: 2191-

2218.

Gascard, J.C., 1973. Vertical motions in the region of deep water formation. *Deep-Sea Res.*, *20*, 11: 1011-1027.

Gascard, J.C., 1978. Mediterranean deep water formation, baroclinic instability and ocean eddies. *Oceanol. Acta*, *1*, 3: 315-330.

Kinder, T.H., and G. Parilla, 1987. Yes, some of the Mediterranean Outflow does come from great depth, *J. Geophys. Res.*, *92*, 2901-2906.

Korres, G., N. Pinardi, A. Lascaratos, 2000. The ocean response to low frequency interannual atmospheric variability in the Mediterranean Sea. Part I: Sensitivity experiments and energy analysis. *J. Climate*, *13*: 705- 731.

Larichev, V., and I. Held, 1995. Eddy amplitudes and fluxes in a homogenious model of fully developed baroclinic instability., *J. Phys. Oceanogr.*, *25*, 2285 - 2297.

Leaman, K.D, and F.A. Schott, 1991. Hydrographic structure of the convective regime in the Gulf of Lions: winter 1987, *J. Phys. Oceanogr*, *21*, N4: 575 - 598.

Legg, S., and J. McWilliams, 2001. Convective modification of a geostrophic eddy field, *J. Phys. Oceanogr*, 31, 874-891.

Legg, S., and J. Marshall, 1993. A heton method of spreading phase of open-ocean deep convection water masses, *J. Phys. Oceanogr*, 23, 1040-1056.

Legg, S., and J. Marshall, 1998. The influence of the ambient flow on the spreading of convective water masses, *J. Mar. Res.*, 56, 107-139.

Madec G., M. Chartier, P. Delecluse, and M. Crepon, 1991. A three-dimensional numerical study of deep-water formation in the northwestern Mediterranean Sea, *J. Phys. Oceanogr.*, *21*: 1349-1371.

Madec G., F. Lott, P. Delecluse, and M. Crepon, 1996. Large-scale preconditioning of deep-water formation in the northwestern Mediterranean Sea, *J. Phys. Oceanogr.*, *26*: 1393 - 1408.

Marshall, J., and F. Schott, 1999. Open-ocean convection: observations, theory, and models, *Rev. Geophys.*, *37*, 1:1-64.

MEDOC Group, 1970. Observations of formation of deep-water in the Mediterranean Sea, 1969, *Nature*, *227*:1037-1040.

Millot C., 1985. Some features of the Algerian Current, *J. Geophys. Res.*, *90*, 7169-7176.

Millot C., 1999. Circulation in the Western Mediterranean Sea. *J. Mar. Syst.*, *20*, 3-4: 423-442.

Millot C., 1994. Models and data: a synergetic approach in the western Mediterranean Sea. In P. Malanotte-Rizzoli and A. R. Robinson Eds., *Ocean Processes in Climate Dynamics: Global and Mediterranean Examples*: 143-149.

Millot C., 1987. Circulation in the Western Mediterranean. *Oceanol. Acta*, *10*, 2: 143-149.

Millot C., M. Benzhora, I. Taupier-Letage, 1997. Circulation in the Algerian Basin inferred from the MEDIPROD-5 current meters data. *Deep-Sea Res.*, *44*: 1467- 1495.

Millot C., I. Taupier-Letage, 2005. Circulation in the Algerian additional evidence of LIW entrainment across the Algerian Basin by mesoscale eddies and not by a permanent westward flow, *Prog. Oceanogr.*, (in press).

Ovchinnikov, I.M., 1966. Circulation in the surface and intermediate layers of the Mediterranean, *Oceanology*, *6*: 48-59.

Pinot, J.-M., J.L. Lopez-Jurado, and M. Riera, 2002. The CANALES experiment (1996-1998). Interannual, seasonal and mesoscale variability of the circulation in the Balearic

Channels, *Progr. Oceanogr.*, *55*, 335-370.

Pinot, J.M., J. Tintore, and D. Gomis, 1995. Multivariate analysis of surface circulation in the Balearic Sea. *Prog. Oceanogr.*, *36*, 343-376.

Puillat I., I. Taupier-Letage, and C. Millot, 2002. Algerian eddies lifetime can Near 3 years, *J. Mar. Syst.*, *31*, 4, 245-259.

Rhines, P.B., 1975. Waves and turbulence on a beta-plane. *J. Fluid. Mech.*, *69*, 417-443.

Rhines, P.B., 1977. The dynamics of unsetady currents. The Sea, Vol. 6, E.A. Godberg, I.N. McCane, J.J. OB́rien, and J.H. Steele, Eds., Wiley, 189-318.

Robinson, A.R., and M. Golnaraghi, 1994. The physical and dynamical oceanography of the Mediterranean Sea, In. Malanotte-Rizzoli, P., and A.R. Robinson Eds., Proceedings of NATO-ASI, *Ocean processes in Climate Dynamics: Global and Mediterranean Examples*, pp 206-306.

Testor P. and J.-C. Gascard, 2003: Large scale spreading of deep waters in the Western Mediterranean Sea by submesoscale coherent eddies, *J. Phys. Oceanogr.*, 33, 75-87.

Testor, P., U. Send, J.-C. Gascard, C. Millot, I. Taupier-Letage, K. Beranger, 2005. The Mean circulation of the southwestern Mediterranean Sea - the Algerina Gyres, *J. Geophys. Res.*, (in press)

Wolfgang Roether, Beniamino B. Manca, Birgit Klein, Davide Bregant, Dimitrios Georgopoulos, Volker Beitzel, Vedrana Kovaevi, Anna Luchetta, 1996. Recent Changes in Eastern Mediterranean Deep Waters, *Science*, *271*, 5247, 333-335.

Roussenov, V., E. Stanev, V. Artale and N. Pinardi, 1995. A seasonal model of the Mediterranean Sea circulation. *J. Geophys. Res.*, *100*: 13515-13538.

Salat, J., and J. Font, 1987. Water mass structure near and offshore the Catalan Sea during the winter of 1982 and 1983. *Annales Geophysicae*, *5*: 49-54.

Salmon, R., 1978. Two-layer quasi-geostrophic turbulence in a simple special case. *Geophys. Astrophys. Fluid. Dyn.*, *10*, 25-52.

Schott F., and K.D. Leaman, 1991. Observations with moored acoustic Doppler current profilers in the convection regime in the Golfe du Lion, *J. Phys. Oceanogr.*, *21*: 558-574.

Schott F., M. Visbeck, U. Send, J. Fischer, L. Stramma, and Y. Desaubies, 1996. Observations of deep convection in the Gulf of Lions, northern Mediterranean, during winter 1991/92, *J. Phys. Oceanogr.*, *26*: 505-524.

Spall, M.A., 2000. Generation of strong messocale eddies by weak ocean gyres. *J. Mar. Res.*, *58*: 97-116.

Swallow,J.C. and G.F. Caston, 1972. The preconditioning phase of MEDOC 1969-I. Observations, Deep-Sea Re., Vol. 20, pp. 429-448.

Vignudelli, S., 1997. Potential use of ERS-1 and Topex/Poseidon altimeters for resolving oceanographic patterns in the Algerian Basin. *Geophys. Res. Lett.*, *24* (14): 1787-1790.

Wu P., and K. Haines, 1996. Modelling the dispersal of Levantine intermediate water and its role in Mediterranean deep water formation, *J. Geophys. Res.*, *101*, C3: 6591 - 6607.

Figure 1. Scheme of the basin-scale circulation in the Mediterranean Sea (after Pinardi and Massetti, 2000).

Fig.2 Botom topography in the Algerian and Ligurian - Provencal basins. The two squared areas shown in the Gulf of Lions and the Algerain Basin are the areas, where energitic analysis is performed in section 6.

Fig.3 Mean velocity and density distributions in the Gulf of Lionss for the period 1-3 January, 1987 at (a)50m; (b) 500m; (c) 1000m; (d) 1800m

Fig.4 Mean velocity and density distributions in the Gulf of Lionss for the period 1-3 January, 1992 at (a)50m; (b) 500m; (c) 1000m; (d) 1800m

Fig.5. Horizontal and veritical extent of the mixed patch in 1987 (after Schott and Leaman, 1991, and Leaman and Schott, 1991). The horizontal extent is shown on upper pannel for (a) 22-29 January, (b) 23-29 January, and (c) 17-23 February, 1987. The density cross section along 5^oE is shown on (d).

Fig.6 Horizontal and veritical extent of the deep convection area in 1992 (after Schott *et al.*, 1996). The horizontal extent and depths are ploted on the upper pannel for (a) 18-22 Frbruaty, 1992, (b) 23 February - 3 March, 1992, and (c) 3-9 March, 1992. The solid line indicates the horizontal boundaries of the surface convectively mixed layer. The numbers on the solid line show depth of the convection. The dashed line show the extension of the convection waters below a stratified layer and the numbers corresponidng to these lines - the depth of the convection water. The density cross section along 5^oE is shown on the lower pannel.

Fig.7 Vertical section of the density along the longitude 5^oE (a) 21-24 February, 1987; (b) 19-21 February, 1992.

Fig.8 Monthly mean horizontal distribution of density and velocity fields at 50 m (a) March, 1987; (b) April, 1987; (c) May 1987; (d) June 1987; (e) August 1987; (f) October, 1987.

Fig.9 Monthly mean horizontal distribution of density and velocity fields at 50 m (a) March, 1992; (b) April, 1992; (c) May 1992; (d) June 1992; (e) August 1992; (f) October, 1992.

Fig.10 Monthly mean horizontal distribution of density and velocity fields at 500 m (a) March, 1987; (b) April, 1987; (c) May 1987; (d) June 1987; (e) August 1987; (f) October, 1987

Fig.11 Monthly mean horizontal distribution of density and velocity fields at 500 m (a) March, 1992; (b) April, 1992; (c) May 1992; (d) June 1992; (e) August 1992; (f) October, 1992

Fig.12 Monthly mean horizontal distribution of density and velocity fields at 1500 m (a) March, 1987; (b) April, 1987; (c) May 1987; (d) June 1987; (e) August 1987; (f) October, 1987

Fig.13 Synopsis of one-year ELISA experiment. a, c, e, g: NOAA-AVHRR infrared images. b,d,f,h schene of the eddy field together with sampling moorings (Δ), CTD (+) and XBT (x) casts. (after Millot and Taupier-Letage, 2005)

Fig.14 Horizontal distribution of temperature and velocity at 30m in the Algerian Basin in four different periods (a) 27 - 30, July, 1997 ; (b) 25-27 March, 1998; (c) 5-9 May, 1998; (d) 22 - 24 June, 1998.

Fig.15 Horizontal distribution of salinity and velocity at 360 m in the Algerian Basin (a) 27 - 30, July, 1997; (b) 25-27 March, 1998; (c) 5-9 May, 1998; (d) 22 - 24 June, 1998.

Fig.16 3-days mean barotropic kinetic energy spectra curves of the baortopic flow in the Gulf of Lions for (a) winter, (b) spring, (c) summer and (d) autmun. The green curve shows the spectra at the beiginnig of each period, the red line - the spectra at the end of the period.

Fig.17 3-days mean barotropic kinetic energy spectra curves of the barotopic flow in the Algerian Basin for (a) winter, (b) spring, (c) summer and (d) autmun. The green curve shows the spectra at the beiginnig of each period, the red line - the spectra at the end of the period.

Fig.18 Stream function (10^{-6} Sv. kg/m^3) of the (a) mean transport in the intermediate layer; (b) mean transport in the deep layer; (c) eddy-induced transport in the intermediate layer; and (d) eddy-induced transport in the deep layer.

Fig.19 (a) Trajectories of the RAFOS floats at 600 m from July 14, 1997 until June 24, 1998. superimposed on f/H contours. (b) Trajectories of profiling floats drifting at 1200 and 2000. Arrows indicate the drift at depth during 8 days.s (after Testor *et al.*, 2005)

file)

1987;

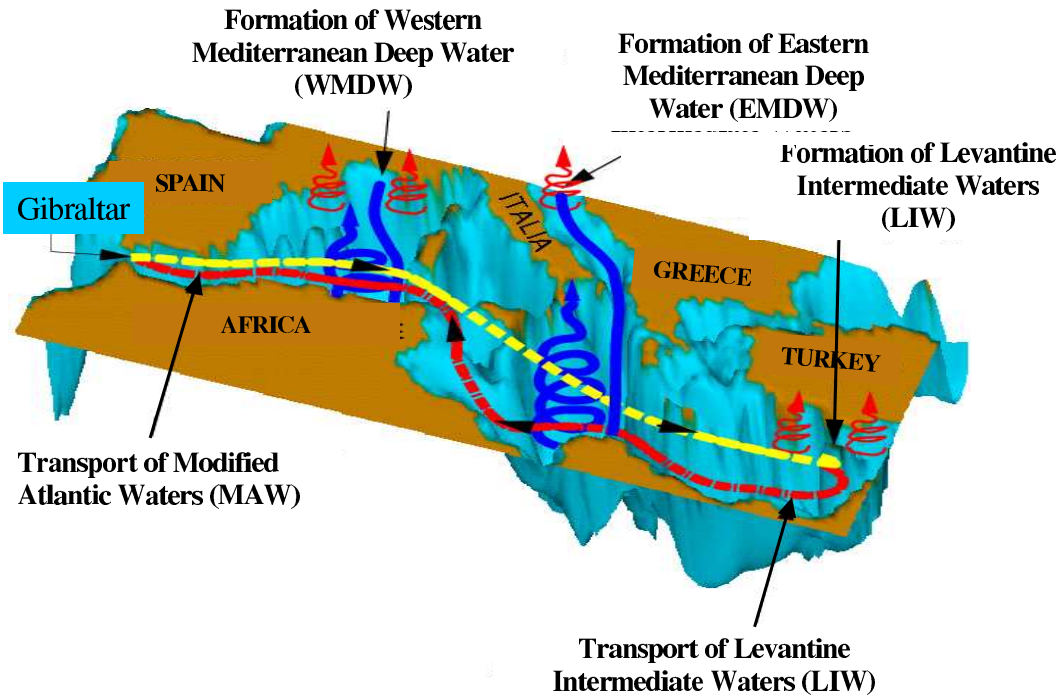

Figure 1. Scheme of the basin-scale circulation in the Mediterranean Sea (after Pinardi and Massetti, 2000).

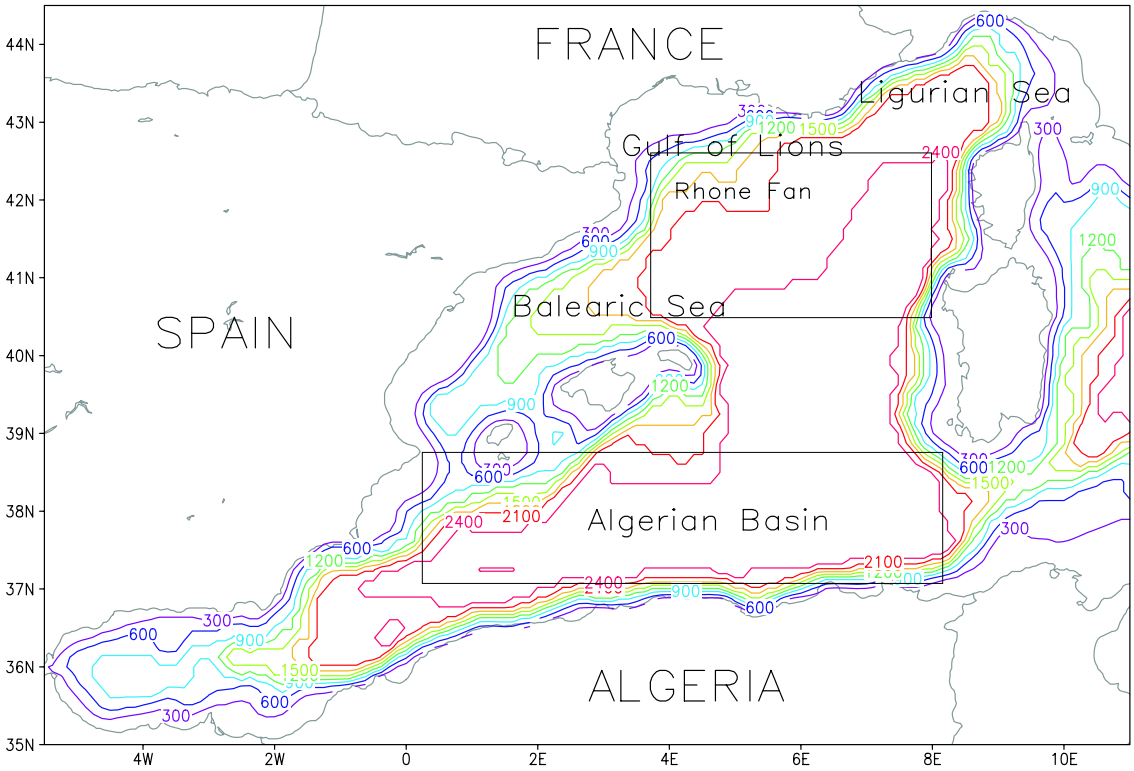

Figure 2. Botom topography in the Algerian and Ligurian - Provencal basins. The two squared areas shown in the Gulf of Lions and the Algerain Basin are the areas, where energitic analysis is performed in section 6.

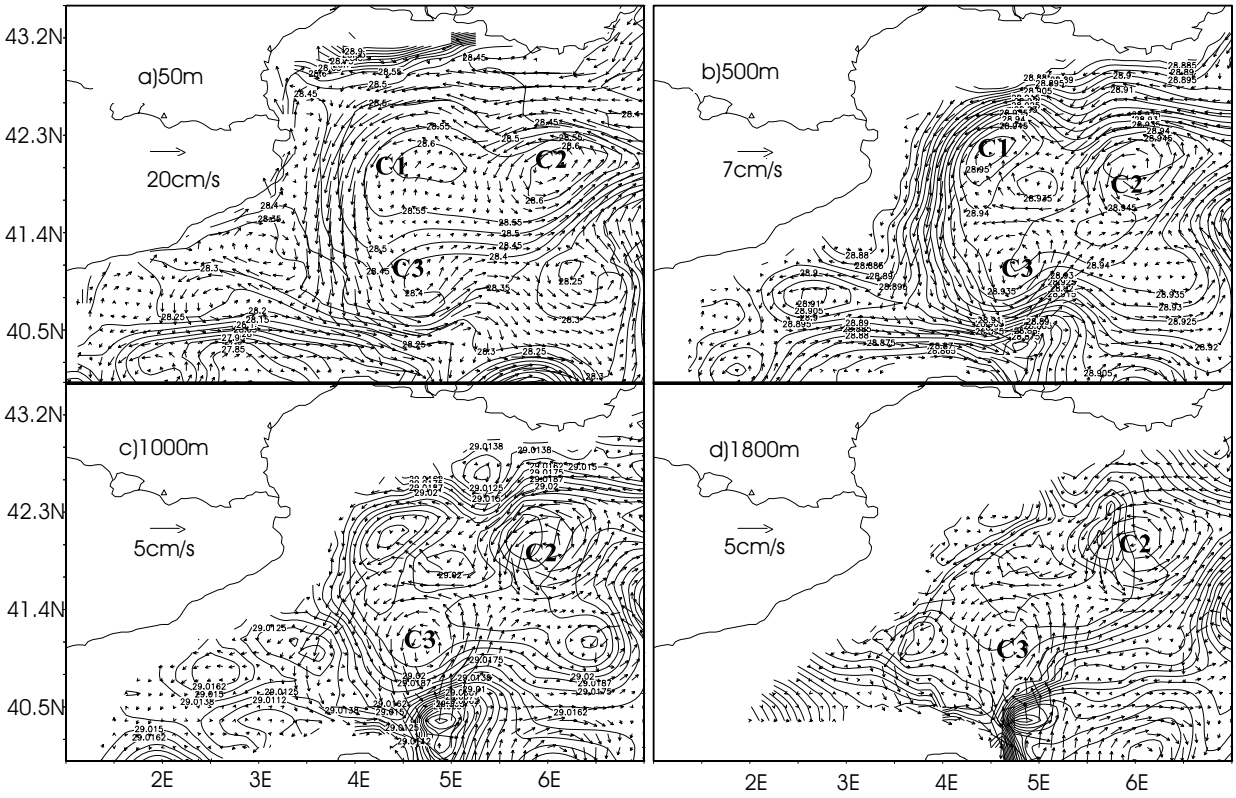

Figure 3. Mean velocity and density distributions in the Gulf of Lionss for the period 1-3 January, 1987 at (a)50m; (b) 500m; (c) 1000m; (d) 1800m

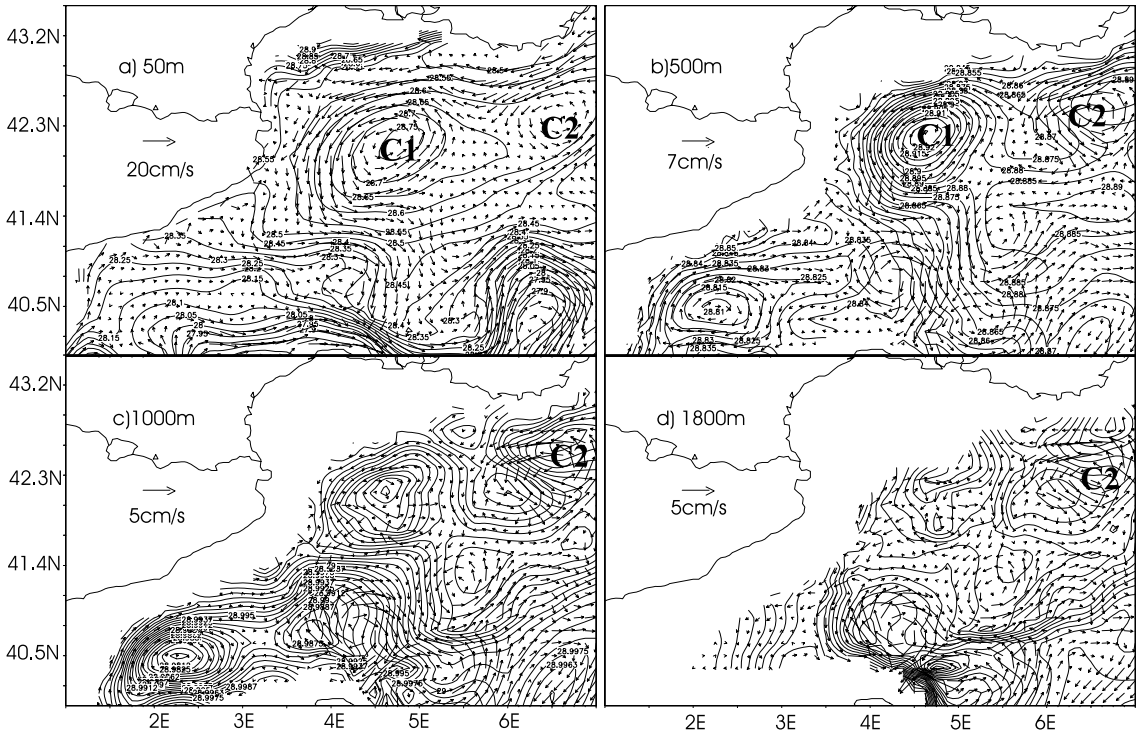

Figure 4. Mean velocity and density distributions in the Gulf of Lionss for the period 1-3 January, 1992 at (a)50m; (b) 500m; (c) 1000m; (d) 1800m

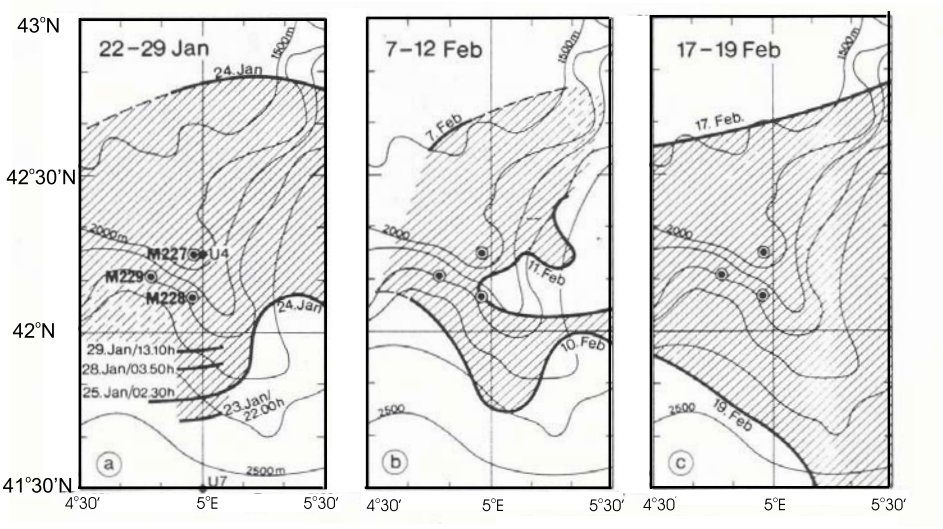

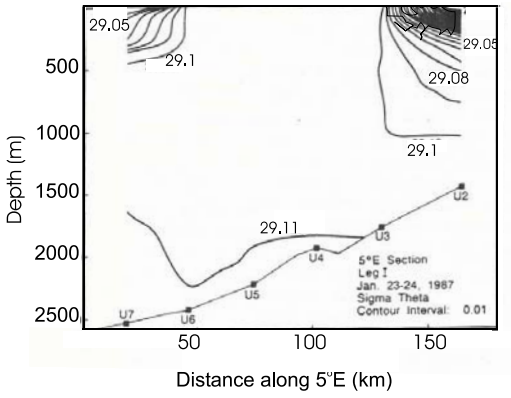

Figure 5. Horizontal and veritical extent of the mixed patch in 1987 (after Schott and Leaman, 1991, and Leaman and Schott, 1991). The horizontal extent is shown on upper pannel for (a) 22-29 January, (b) 23-29 January, and (c) 17-23 February, 1987. The density cross section along 5°E is shown on (d).

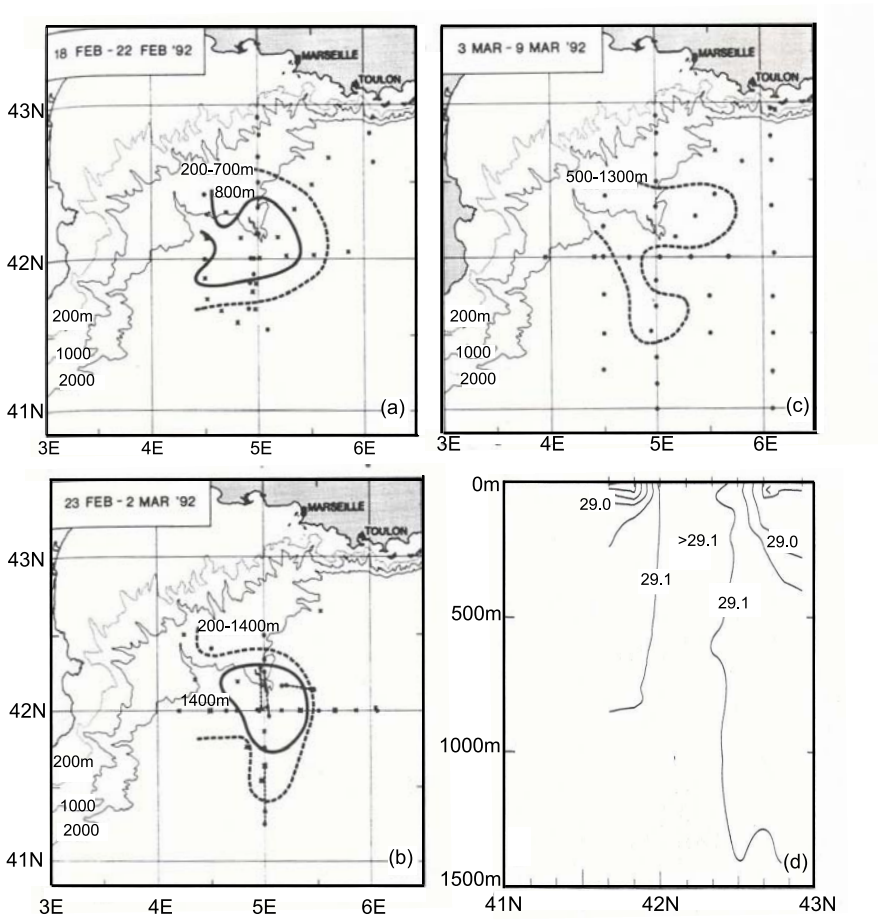

Figure 6. Horizontal and veritical extent of the deep convection area in 1992 (after Schott *et al.*, 1996). The horizontal extent and depths are ploted on the upper pannel for (a) 18-22 Frbruaty, 1992, (b) 23 February - 3 March, 1992, and (c) 3-9 March, 1992. The solid line indicates the horizontal boundaries of the surface convectively mixed layer. The numbers on the solid line show depth of the convection. The dashed line show the

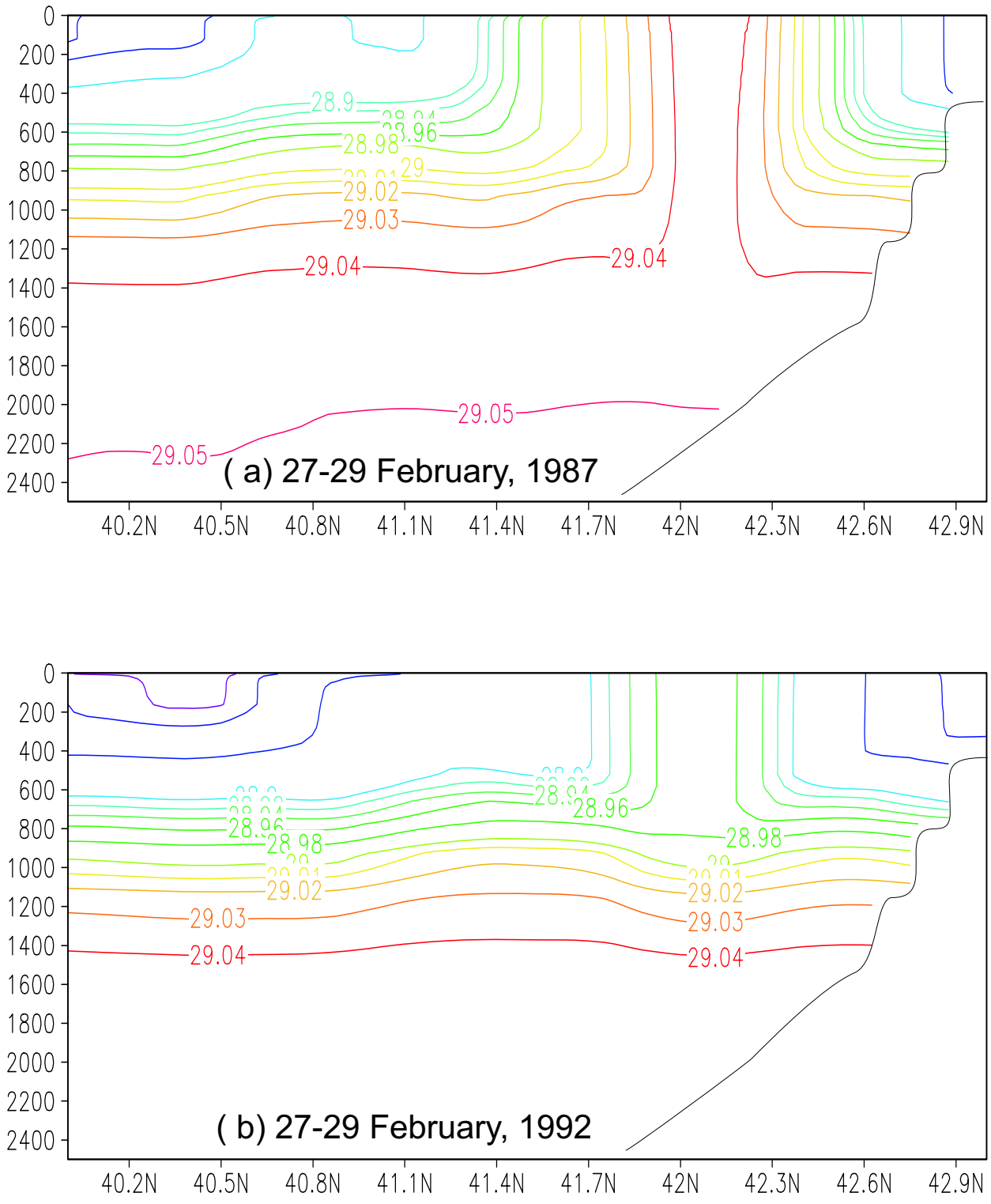

Figure 7. Vertical section of the density along the longitude 5^{o}E (a) 21-24 February, 1987; (b) 19-21 February, 1992

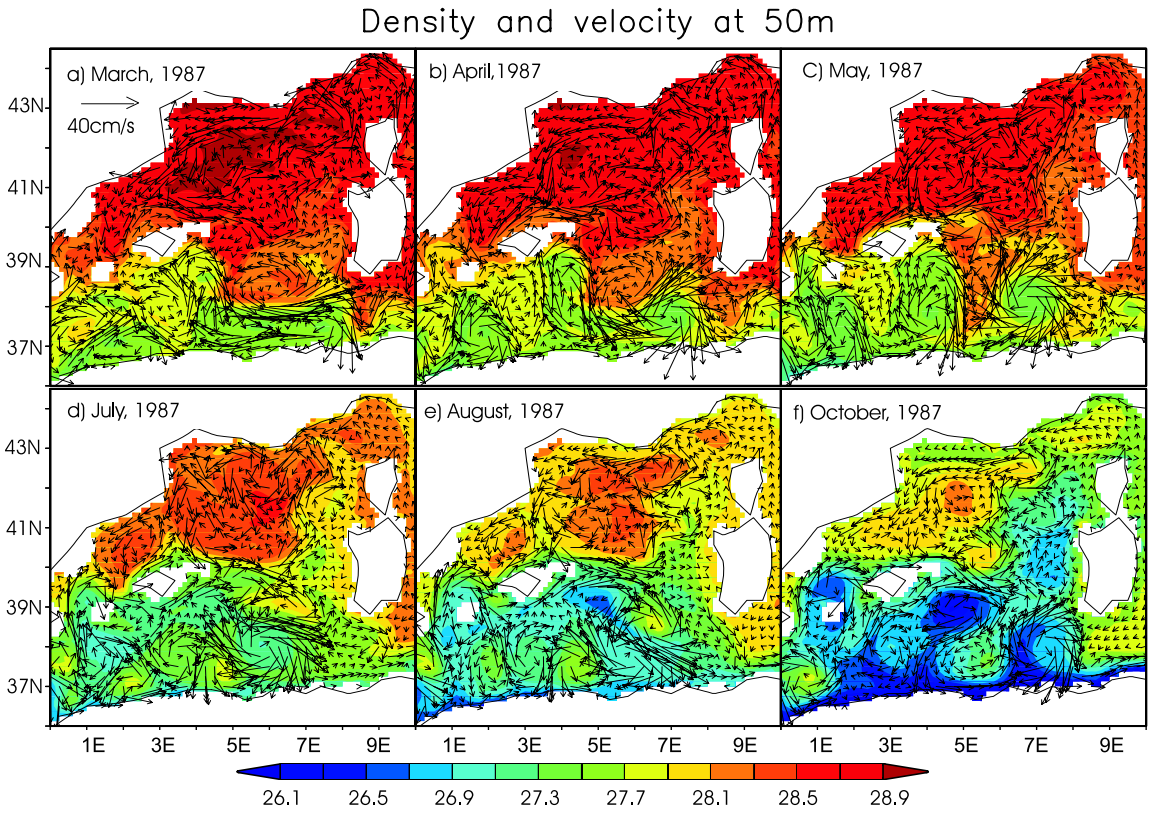

Figure 8. Monthly mean horizontal distribution of density and velocity fields at 50 m (a) March, 1987; (b) April, 1987; (c) May 1987; (d) June 1987; (e) August 1987; (f) October, 1987

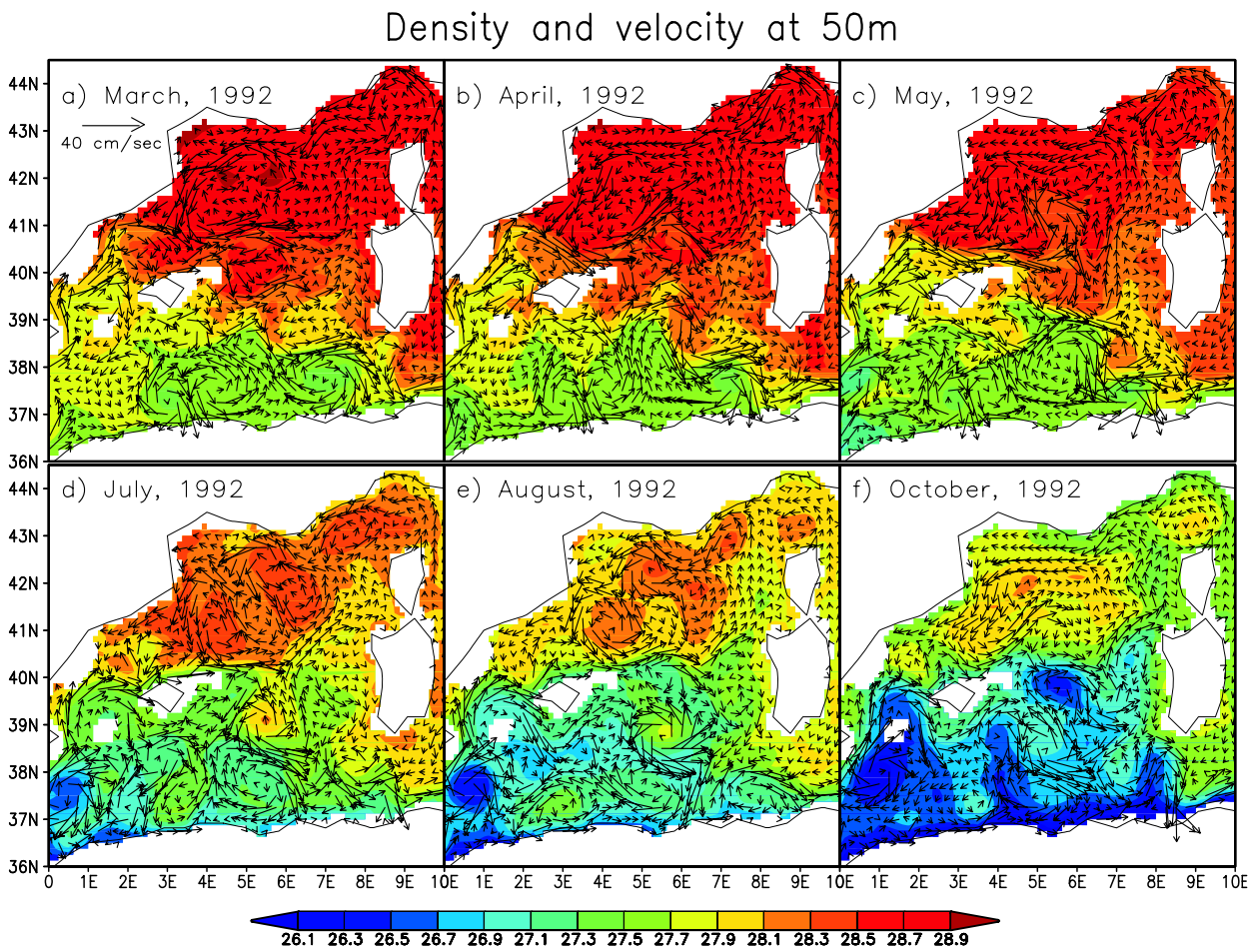

Figure 9. Monthly mean horizontal distribution of density and velocity fields at 50 m (a) March, 1992; (b) April, 1992; (c) May 1992; (d) June 1992; (e) August 1992; (f) October, 1992

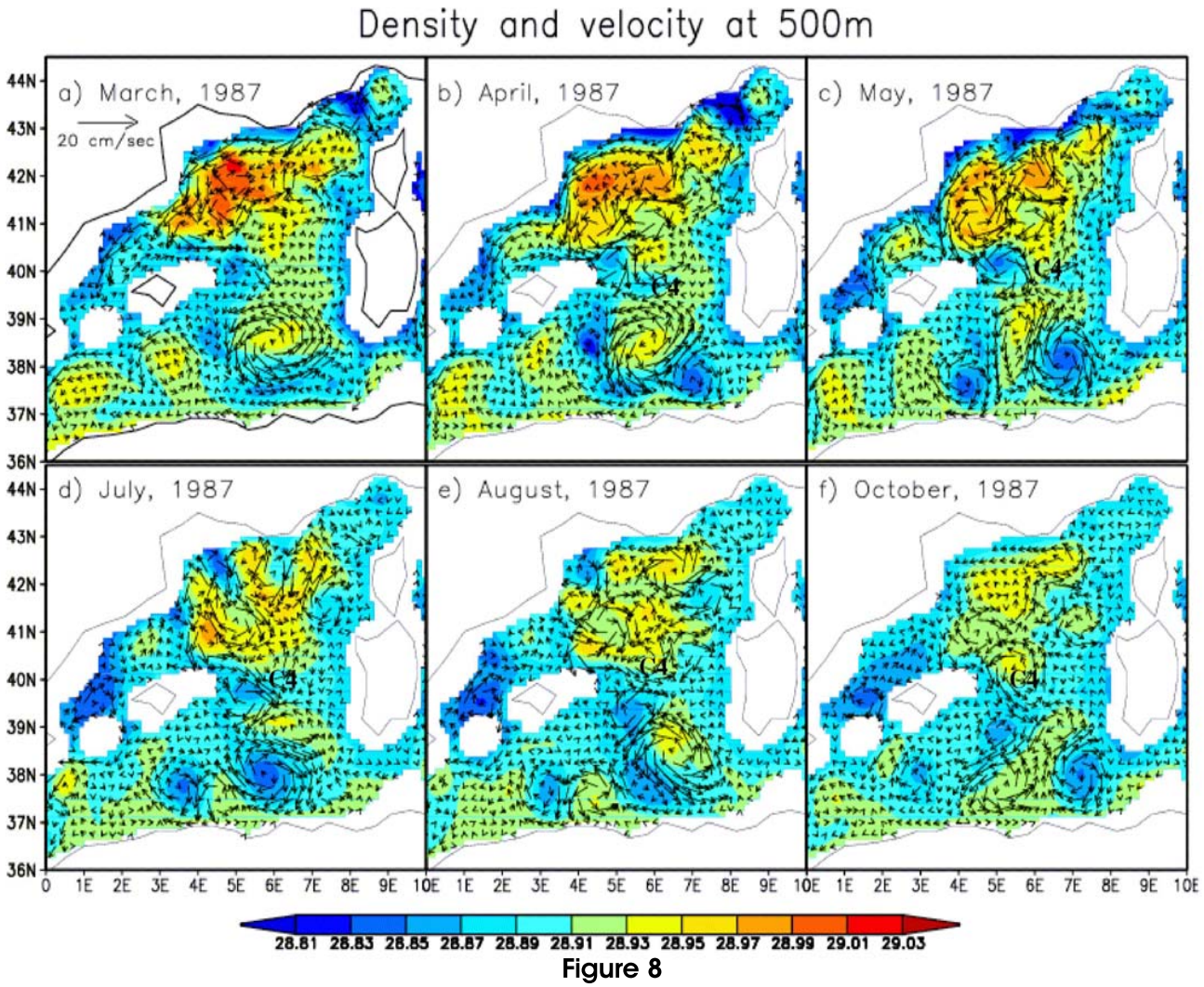

Figure 8

Figure 10. Monthly mean horizontal distribution of density and velocity fields at 500 m (a) March, 1987; (b) April, 1987; (c) May 1987; (d) June 1987; (e) August 1987; (f) October, 1987

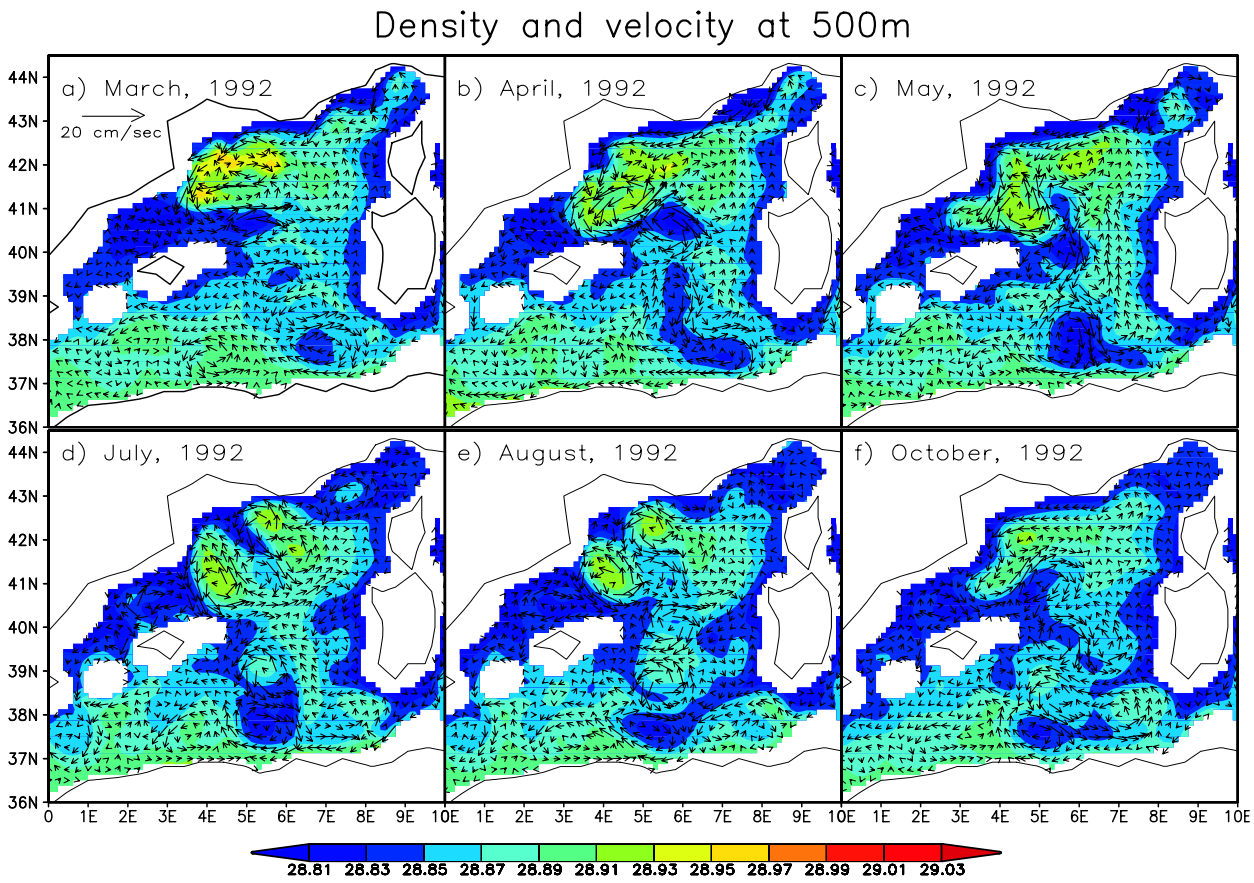

Figure 11. Monthly mean horizontal distribution of density and velocity fields at 500 m (a) March, 1992; (b) April, 1992; (c) May 1992; (d) June 1992; (e) August 1992; (f) October, 1992

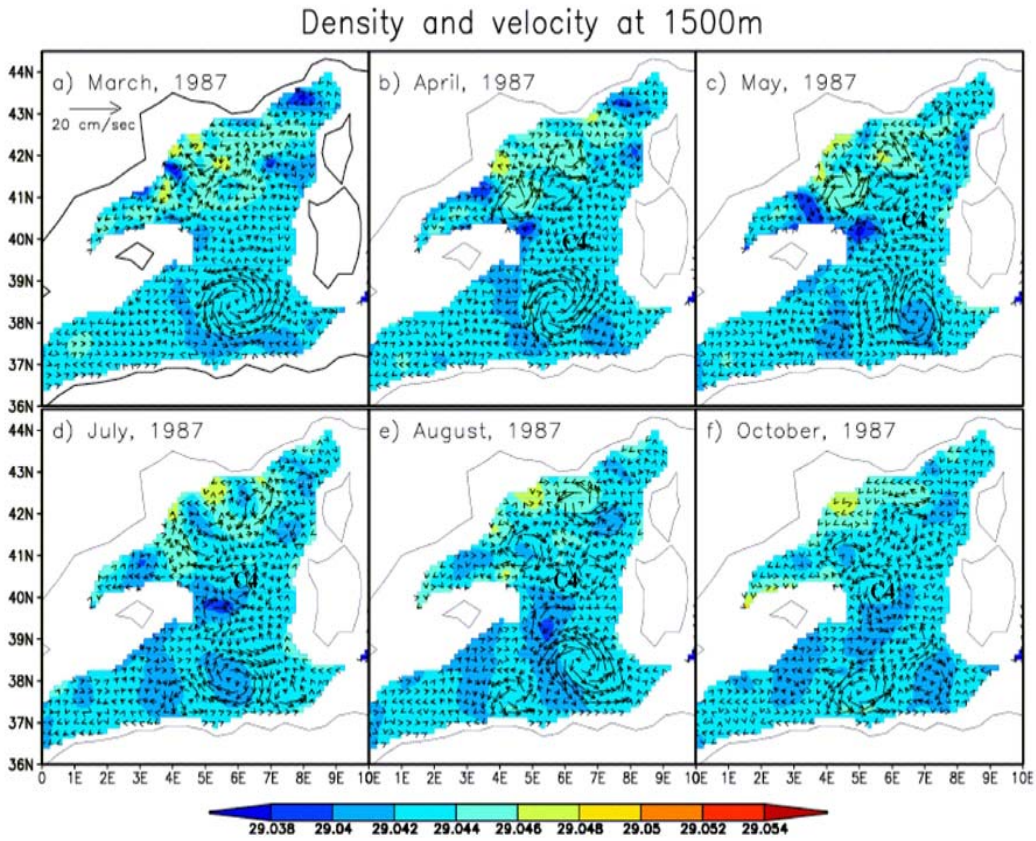

Figure 10

Figure 12. Monthly mean horizontal distribution of density and velocity fields at 1500 m (a) March, 1987; (b) April, 1987; (c) May 1987; (d) June 1987; (e) August 1987; (f) October, 1987

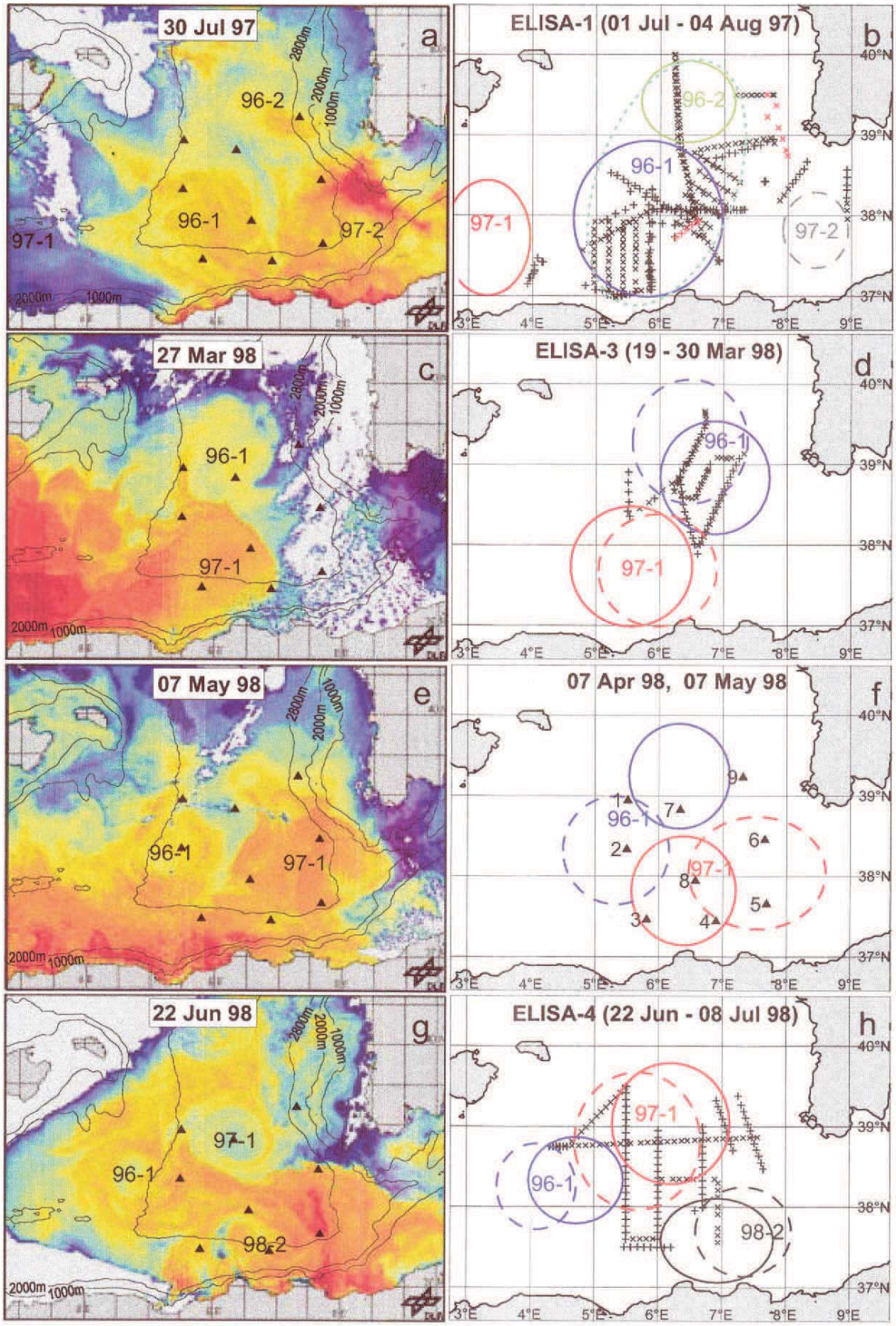

Figure 13. Synopsis of one-year ELISA experiment. a, c, e, g: NOAA-AVHRR infrared images. b,d,f,h schene of the eddy field together with sampling moorings (Δ), CTD (+)

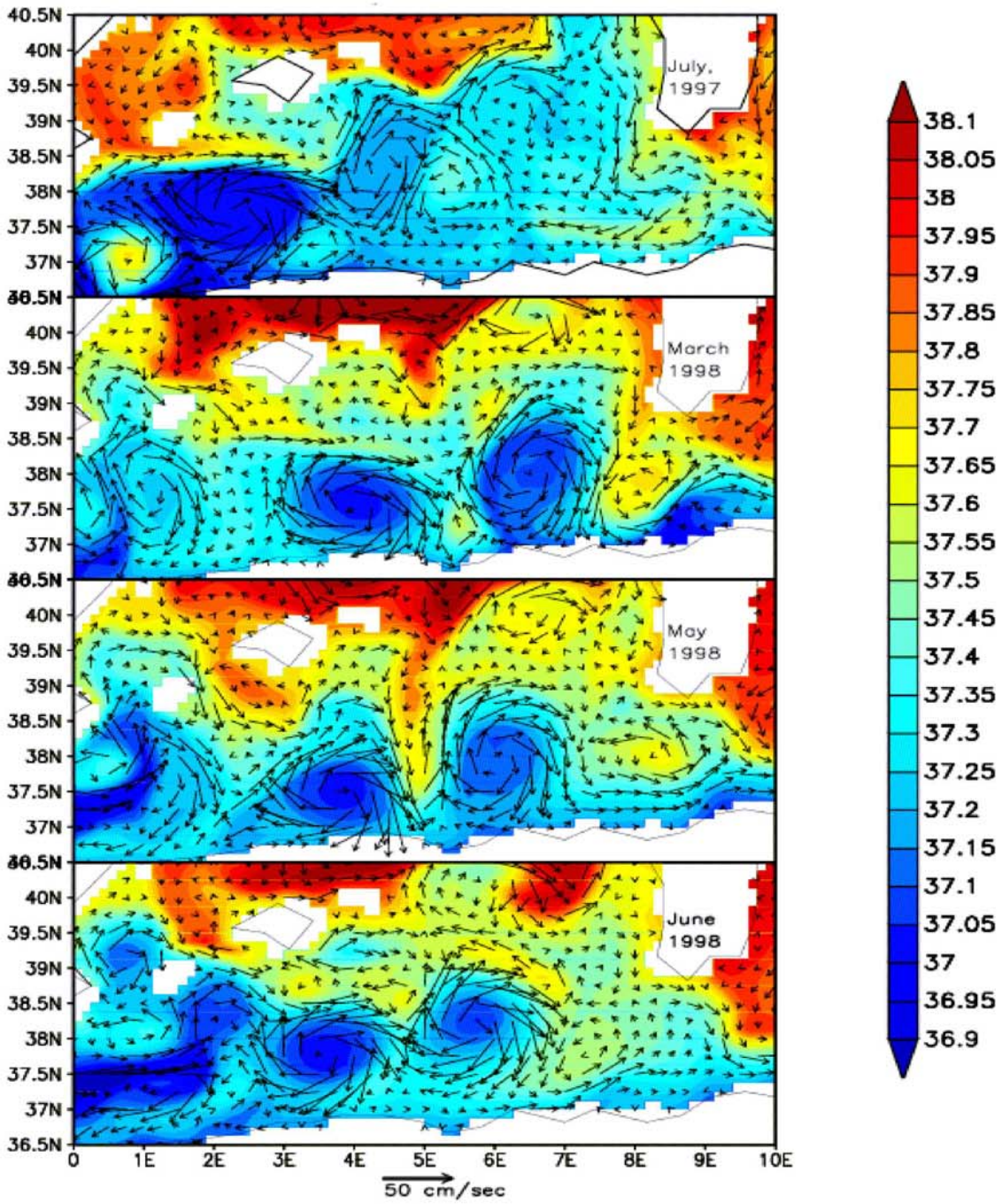

Figure 12

Figure 14. Horizontal distribution of temperature and velocity at 30m in the Algerian Basin in four different periods (a) 27 - 30, July, 1997 ; (b) 25-27 March, 1998; (c) 5-9 May, 1998; (d) 22 - 24 June, 1998.

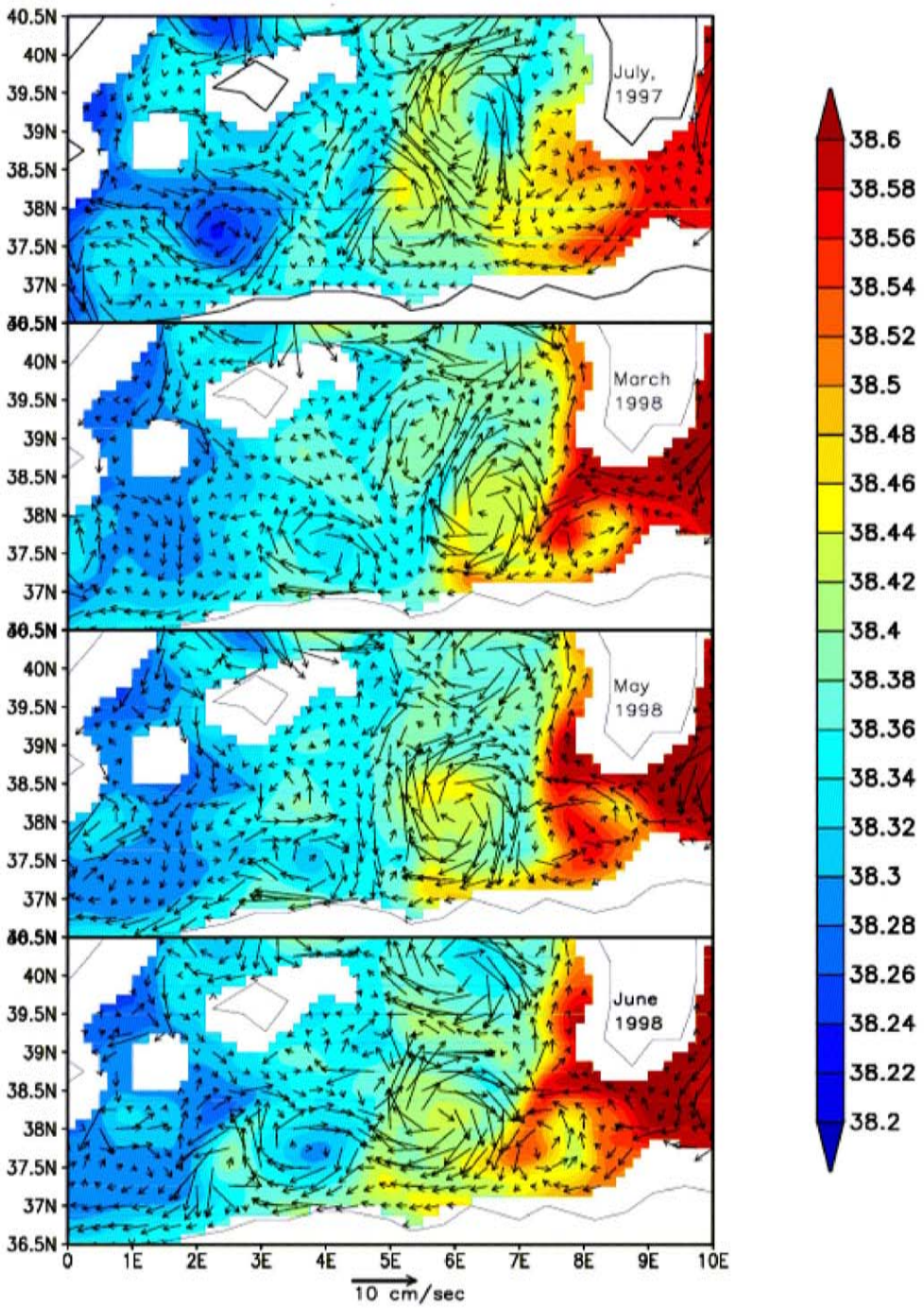

Figure 13

Figure 15. Horizontal distribution of salinity and velocity at 360 m in the Algerian Basin (a) 27 - 30, July, 1997; (b) 25-27 March, 1998; (c) 5-9 May, 1998; (d) 22 - 24 June, 1998.

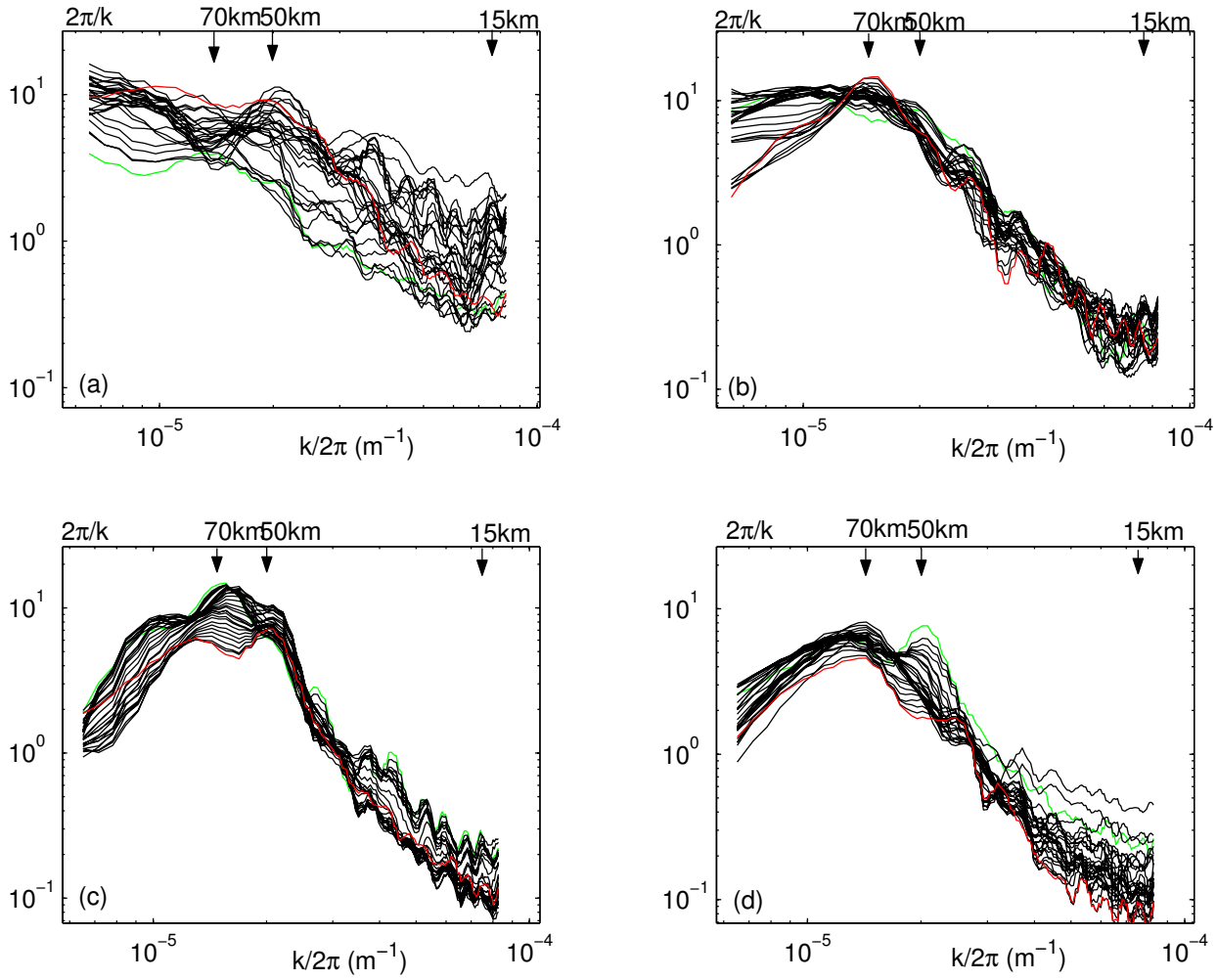

Figure 16. 3-days mean barotropic kinetic energy spectra curves of the baortopic flow in the Gulf of Lions for (a) winter, (b) spring, (c) summer and (d) autmun. The green curve shows the spectra at the beiginnig of each period, the red line - the spectra at the end of the period.

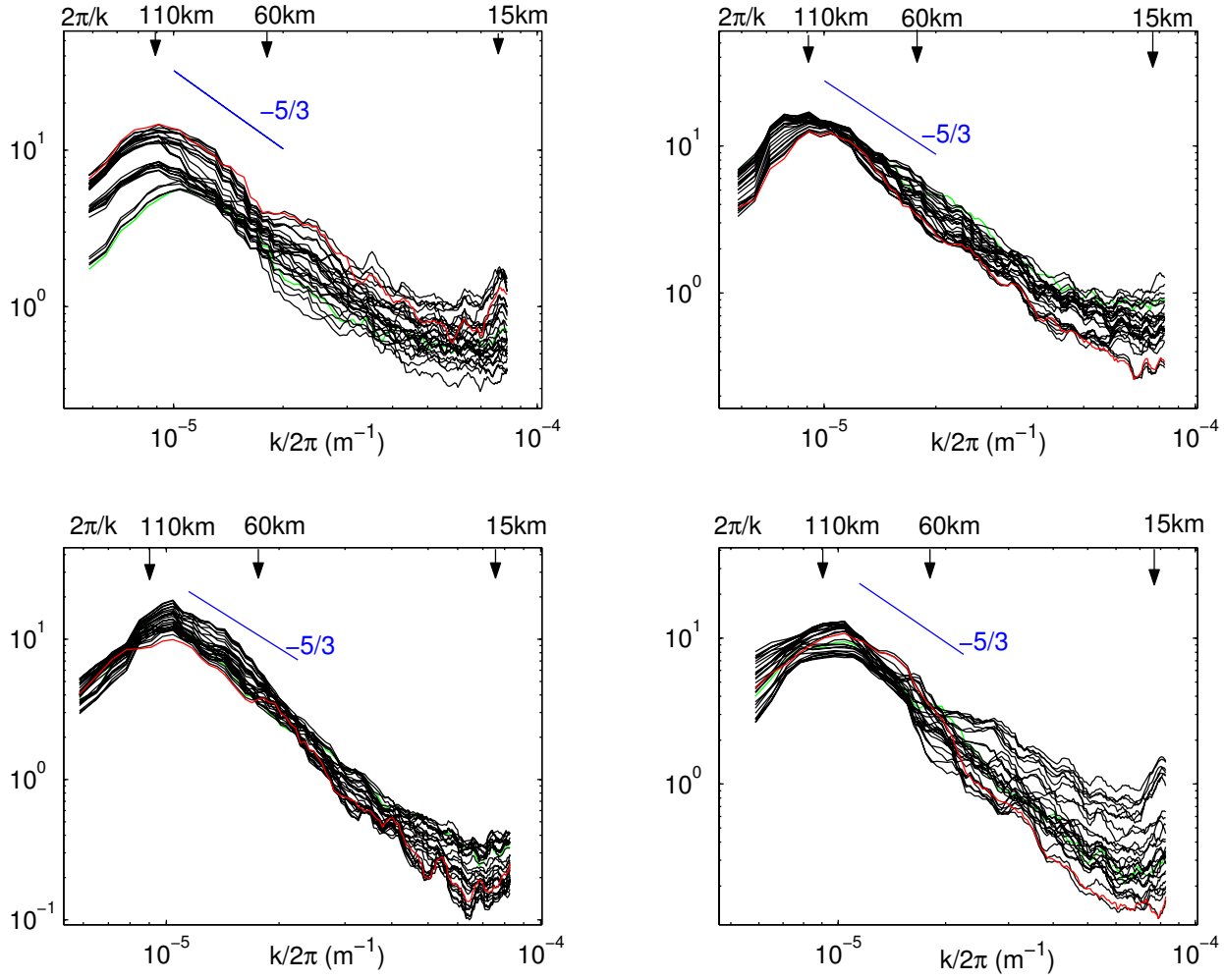

Figure 17. 3-days mean barotropic kinetic energy spectra curves of the barotopic flow in the Algerian Basin for (a) winter, (b) spring, (c) summer and (d) autmun. The green curve shows the spectra at the beiginnig of each period, the red line - the spectra at the end of the period.

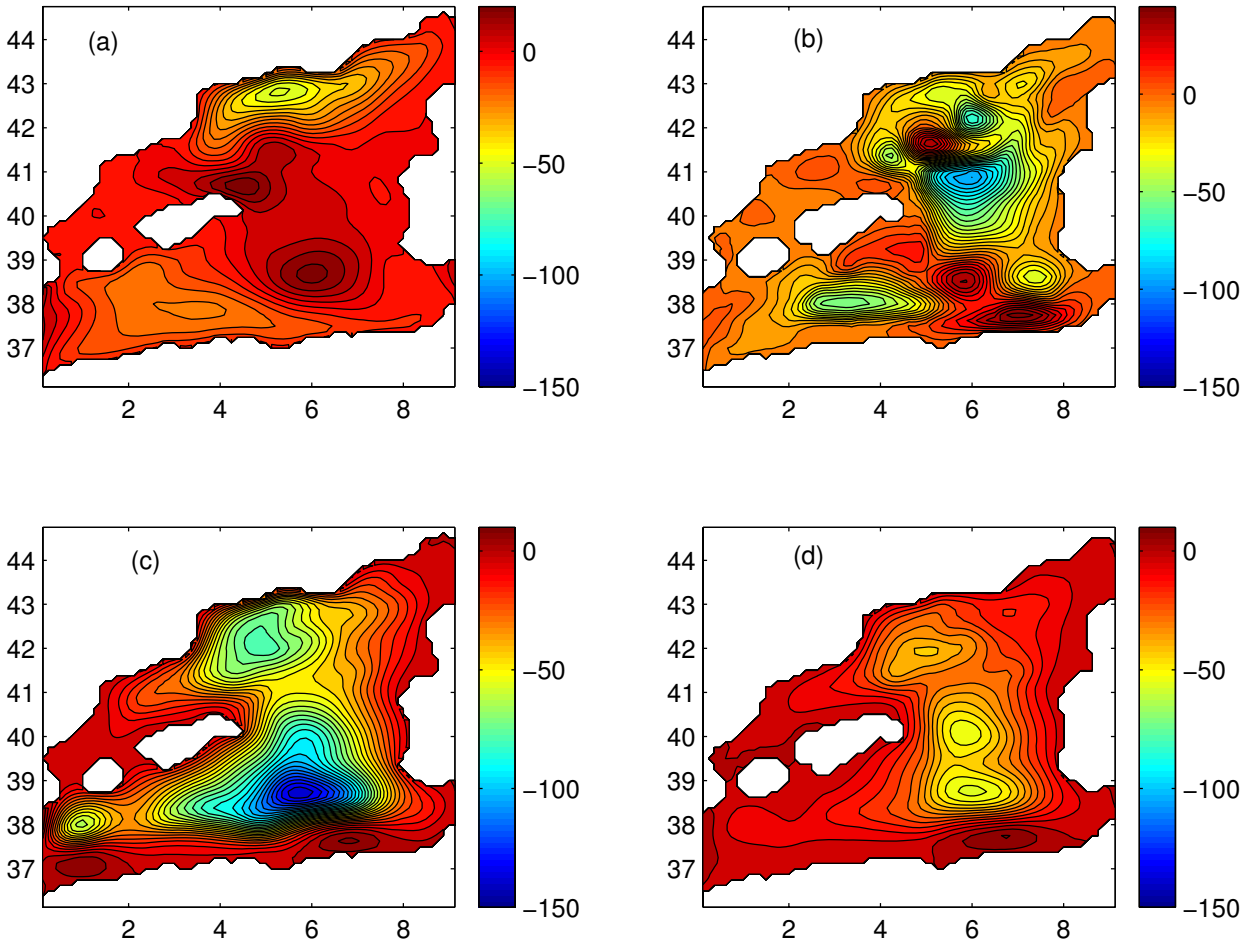

Figure 18. Stream function (10^6 Sv. kg/m^3) of the (a) mean transport in the intermediate layer; (b) mean transport in the deep layer; (c) eddy-induced transport in the intermediate layer; and (d) eddy-induced transport in the deep layer.

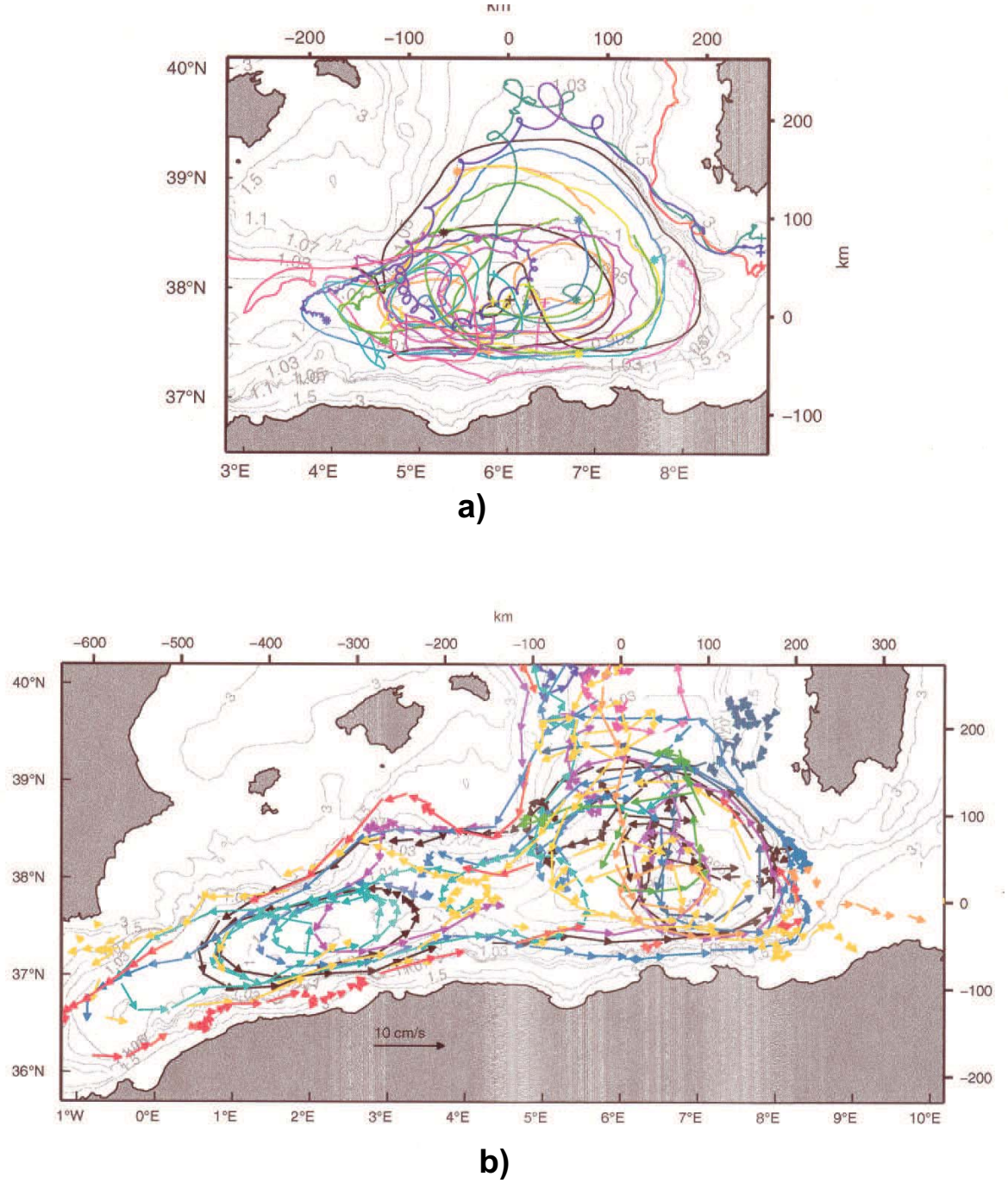

Figure 19. (a) Trajectories of the RAFOS floats at 600 m from July 14, 1997 until June 24, 1998. superimposed on f/H contours. (b) Trajectories of profiling floats drifting at 1200 and 2000. Arrows indicate the drift at depth during 8 days.s (after Testor *et al.*, 2005)

Table 1. Components of energy balance in the surface layer of Gulf of Lions

Parameter	Winter	Spring	Summer	Autumn
$KE_m[J/m^3]$	2.77	3.40	2.13	1.87
$KE_e[J/m^3]$	2.63	4.54	3.80	3.83
$APE_m[J/m^3]$	674.79	85.09	27.89	23.69
$APE_e[J/m^3]$	853.06	17.99	12.41	26.35
$T_1[10^{-7}W/m^3]$	-318.67	-41.36	-16.7	-14.42
$T_2[10^{-7}W/m^3]$	-4.02	-3.39	-6.15	-4.55

Table 2. Components of energy balance in the intermediate layer of Gulf of Lions

Parameter	Winter	Spring	Summer	Autumn
$KE_m[J/m^3]$	0.45	0.93	0.40	0.29
$KE_e[J/m^3]$	0.77	1.58	1.11	0.81
$APE_m[J/m^3]$	31.13	26.53	28.59	32.35
$APE_e[J/m^3]$	7.91	7.29	8.00	7.14
$T_1[10^{-7}W/m^3]$	-14.05	-19.86	-11.66	-4.33
$T_2[10^{-7}W/m^3]$	-0.33	-0.55	-0.42	-0.35

Table 3. Components of energy balance in the deep layer of Gulf of Lions

Parameter	Winter	Spring	Summer	Autumn
$KE_m[J/m^3]$	0.09	0.19	0.08	0.05
$KE_e[J/m^3]$	0.37	0.83	0.52	0.42
$APE_m[J/m^3]$	831.29	815.26	819.15	829.20
$APE_e[J/m^3]$	1.93	2.24	1.92	1.74
$T_1[10^{-7}W/m^3]$	-1.09	-2.39	-0.81	-0.51
$T_2[10^{-7}W/m^3]$	0.13	0.07	-0.05	0.04

Table 4. Components of energy balance in the surface layer of the Algerian Basin

Parameter	Winter	Spring	Summer	Autumn
$KE_m[J/m^3]$	1.89	2.07	2.22	1.36
$KE_e[J/m^3]$	10.17	12.56	11.52	8.43
$APE_m[J/m^3]$	3860.73	613.74	221.03	136.82
$APE_e[J/m^3]$	950.43	129.21	73.90	63.97
$T_1[10^{-7}W/m^3]$	-1251.78	-174.70	-10.63	-41.65
$T_2[10^{-7}W/m^3]$	-9.49	-4.31	5.95	-11.59

Table 5. Components of energy balance in the intermediate layer of the Algerian Basin

Parameter	Winter	Spring	Summer	Autumn
$KE_m[J/m^3]$	0.12	0.15	0.21	0.13
$KE_e[J/m^3]$	1.12	1.40	1.40	1.07
$APE_m[J/m^3]$	69.29	71.00	69.43	65.50
$APE_e[J/m^3]$	10.45	12.03	10.71	9.13
$T_1[10^{-7}W/m^3]$	-1.58	-1.26	-0.67	-0.57
$T_2[10^{-7}W/m^3]$	-0.20	-0.32	0.23	-0.21

Table 6. Components of energy balance in the deep layer of the Algerian basin

Parameter	Winter	Spring	Summer	Autumn
$KE_m[J/m^3]$	0.03	0.04	0.11	0.11
$KE_e[J/m^3]$	0.63	0.74	0.75	0.61
$APE_m[J/m^3]$	896.99	893.47	882.94	885.75
$APE_e[J/m^3]$	1.26	1.33	1.30	1.28
$T_1[10^{-7}W/m^3]$	-0.10	-0.07	-0.03	-0.05
$T_2[10^{-7}W/m^3]$	-0.00	-0.09	0.10	-0.13